

Antineutrino reactor safeguards – a case study

Eric Christensen, Patrick Huber[†], Patrick Jaffke

Center for Neutrino Physics, Virginia Tech, Blacksburg, VA 24061, USA

Abstract

Antineutrinos have been proposed as a means to safeguard nuclear reactors for more than 30 years and there has been impressive experimental progress in antineutrino detection that makes this method increasingly practical for use by the International Atomic Energy Agency. In this paper we conduct, for the first time, a case study of the application of antineutrino safeguards to a real-world scenario – the North Korean nuclear crisis in 1994. We derive detection limits to a partial or full core discharge in 1989 based on actual IAEA safeguards access and find that two independent methods would have yielded positive evidence for a second core with very high confidence. To generalize our results, we provide detailed estimates for the sensitivity to the plutonium content of various types of reactors, including most types of plutonium production reactors, based on detailed reactor simulations. A key finding of this study is that a wide class of reactors with a thermal power of 0.1-1 GW_{th} can be safeguarded achieving IAEA goals for quantitative sensitivity and timeliness with antineutrino detectors right outside the reactor building. This type of safeguards does not rely on the continuity of knowledge and provides information about core inventory and power status in real-time.

[†]Email:pahuber@vt.edu

Contents

1	Introduction	4
2	Antineutrino reactor safeguards	8
2.1	Neutrino detection	9
2.2	Reactor flux models	11
2.3	Reactor physics	15
2.4	Plutonium content determination	18
3	Summary of the 1994 crisis	22
4	Plutonium production in the DPRK	26
5	Neutrinos in the DPRK case	29
5.1	5 MW _e reactor	31
5.2	IRT reactor	33
5.3	5 MW _e reactor power measurement at IRT	35
5.4	Waste detection	37
5.5	Continuous neutrino observations	38
5.6	Impact of backgrounds	40
6	Application to the 1994 crisis	44
6.1	Conventional methods	44
6.2	Neutrinos	48
7	Summary & Outlook	52
A	The 5 MW_e reactor	59
B	CANDU and LEU reactors	62

1 Introduction

The first use of nuclear weapons in 1945, at the end of World War II, had a profound and permanent impact on foreign relations and international security. While initially there was some hope that the secrets of the manufacture of nuclear weapons would remain exclusively in the hands of the United States, the Soviet Union tested its first nuclear device in 1949. Several times during the Cold War, the world stood at the brink of nuclear armageddon. It was only due to the strong commitment of political leaders on both sides and the high degree of professionalism in the armed forces that the disaster of a nuclear war could be averted ¹. During the Cold War, nuclear security was essentially a bipolar issue between the United States and the Soviet Union; other players like Great Britain (1952), France (1960), and China (1964) appeared at the fringes but did not play a major role for most parts. To some degree independently of Cold War politics, Israel and South Africa launched a nuclear weapons program in the early 60s and 70s, respectively, which in both cases was triggered by unique national security needs – a small minority population surrounded by hostile neighbors, which in turn resulted in a rather unusual alliance.² South Africa, quite remarkably, relinquished its nuclear weapons and the associated infra-structure towards the end of the apartheid regime in 1991.³ India’s nuclear program was launched quite early and presumably was a direct response to its deteriorating relations with Pakistan. Also confrontations with China over territories in the Himalayas in combination with China obtaining a permanent seat on the UN Security Council contributed significantly to the decision to go nuclear. Obviously, India’s possession of nuclear weapons since 1974, then created a perceived need for nuclear armament in Pakistan, which first tested a nuclear device in 1998. The last country to join the circle of nuclear armed nations was the Democratic People’s Republic of Korea

1. Thomas Reed, *At the Abyss: An Insider’s History of the Cold War* (Presidio Press, 2004). For a different perspective, why we the Cold War remained cold, see for instance Scott D. Sagan, *The Limits of Safety* (Princeton University Press, 1993).

2. Sasha Polakow-Suransky, *The Unspoken Alliance: Israel’s Secret Relationship with Apartheid South Africa* (Pantheon, 2010).

3. James Doyle, ed., “Nuclear Safeguards, Security and Nonproliferation: Achieving Security with Technology and Policy,” in (Butterworth-Heinemann, 2008), chap. 16.

(DPRK) with its first nuclear test in 2006.

The Treaty on the Non-proliferation of Nuclear Weapons (NPT) was opened for signature in 1968, entered into force in 1970, and on May 11, 1995 the NPT was extended indefinitely.⁴ The NPT is, with exception of the UN charter, the most widely accepted international treaty to date. Currently, 190 states are party to the NPT. The legal mechanisms for IAEA safeguards, as set out in article III of the NPT, are bi-lateral agreements between individual member states and the IAEA. These so-called comprehensive safeguards agreements have been put into force by all but 12 of the non-nuclear-weapons states.⁵ The Additional Protocol was introduced in response to the failure of the regular safeguards scheme to provide timely indication of Saddam Hussein's nuclear weapons program before the first Gulf War in 1990. The Additional Protocol in particular provides IAEA inspectors with the right to collect environmental samples at locations outside of declared facilities and to obtain access to sites which have not been declared as nuclear facilities but are suspected to be. These provisions close an important gap in the regular safeguards scheme, which relies on a state's declaration of nuclear facilities and materials. 139 states have signed the Additional Protocol, and 117 states have put it into force.⁶ The regular safeguards scheme could only confirm the correctness of a state's declaration of nuclear activities; with the Additional Protocol, the completeness of the declaration can also be addressed⁷. It can be argued that the correctness aspect of safeguards is working quite well. No case of diversion of fissile material has been documented at safeguarded facilities, which presumably is due to the fact that a potential proliferator deems the risk of discovery to be unacceptably high.⁸ However, the completeness aspect remains troubling, especially for those states which have not put the

4. "NPT," <http://www.un.org/disarmament/WMD/Nuclear/NPTtext.shtml> (accessed November 19, 2013).

5. "NPT status," http://www.iaea.org/Publications/Factsheets/English/nptstatus_overview.html (accessed December 18, 2013).

6. "IAEA webpage," <http://www.iaea.org/newscenter/focus/npt/index.shtml> (accessed September 13, 2012).

7. In principle, special inspections could also provide the means to verify the completeness, independent of whether the Additional Protocol is in force.

8. Sergey Zykov, "IAEA Instrumentation for the Future," in *Proceedings of the 53rd Annual Meeting of the Institute for Nuclear Materials Management (INMM)* (2012).

additional protocol into force, such as Iran.

Neutrinos were postulated by Wolfgang Pauli in 1930 and have been experimentally discovered by Clyde Cowan and Fred Reines⁹ in 1956 using neutrinos¹⁰ from the Savannah River reactor. Neutrinos are nearly massless, electrically neutral, spin 1/2 particles and play a central role in the electroweak Standard Model of particle physics. Neutrinos participate only in weak interactions and therefore possess unusual penetrating power – no practical means to attenuate or to shield neutrinos are known. Neutrinos are copiously produced in the beta-decays of fission fragments and this makes nuclear reactors the most powerful artificial neutrino source. The basic concept to monitor nuclear reactors using neutrinos was proposed by Borovoi and Mikaelyan in 1978.¹¹ There have been a number of quantitative studies of the level of accuracy at which the plutonium content in a reactor can be determined using neutrinos,¹² and different authors seem to come to different conclusions. Closer inspection of those results reveal that very different assumptions about detector capabilities are made and also the level of statistical analysis, particularly in terms of rates versus spectral information, is very different. These differences likely account for the variety of opinions on the feasibility and quantitative accuracy of neutrino safeguards. In particular, the assumptions about detector capabilities seem to be strongly influenced by earlier safeguards detector deployments and do not reflect modern state-of-the-art neutrino detectors. We will

9. C. L. Cowan et al., “Detection of the free neutrino: A Confirmation,” *Science* 124 (1956): 103–104, doi:10.1126/science.124.3212.103.

10. To be precise, a reactor is a source of electron antineutrinos. In the interest of brevity and given the fact that here we are dealing only with electron antineutrinos, we will use the term neutrino, instead.

11. A. A. Borovoi and L. A. Mikaelyan, “Possibilities of the practical use of neutrinos,” *Soviet Atomic Energy* 44 (1978): 589.

12. Adam Bernstein et al., “Nuclear reactor safeguards and monitoring with anti-neutrino detectors” (2001); Michael Martin Nieto et al., “Detection of anti-neutrinos for nonproliferation” (2003); Patrick Huber and Thomas Schwetz, “Precision spectroscopy with reactor anti-neutrinos,” *Phys. Rev. D* 70 (2004): 053011, doi:10.1103/PhysRevD.70.053011; A.C. Misner, “Simulated Antineutrino Signatures of Nuclear Reactors for Nonproliferation Applications” (PhD diss., Oregon State University, 2008); A. Bernstein et al., “Nuclear Security Applications of Antineutrino Detectors: Current Capabilities and Future Prospects,” *Sci.Global Secur.* 18 (2010): 127–192; Vera Bulaevskaya and Adam Bernstein, “Detection of Anomalous Reactor Activity Using Antineutrino Count Rate Evolution Over the Course of a Reactor Cycle,” *J.Appl.Phys.* (2010); A.C. Hayes et al., “Theory of Antineutrino Monitoring of Burning MOX Plutonium Fuels,” *Phys.Rev.* C85 (2012): 024617, doi:10.1103/PhysRevC.85.024617; Patrick Huber, “Spectral antineutrino signatures and plutonium content of reactors,” in *Proceedings of the 53rd Annual Meeting of the Institute for Nuclear Materials Management (INMM)* (2012).

discuss these issues in detail in section 2. We will not discuss the application of neutrinos for long-range detection of nuclear activities¹³.

Here, we present the first case study of a real safeguards scenario – the first nuclear crisis in the DPRK in 1994.¹⁴ Earlier studies of neutrinos for safeguards are, to a large degree, based on pre-conceived notions of how safeguards of a particular reactor type work, and thus do not allow critical examination of the strength and weaknesses of neutrino safeguards as compared to more conventional means. In many cases, this comparison seems to disfavor neutrinos, not because neutrinos do not offer any new capabilities, but because the conventional techniques are specifically designed to work well in those standard scenarios.¹⁵ On the other hand, inventing scenarios in which the standard methods fail brings about the criticism that these scenarios are artificial, unrealistic, and contrived for the sole purpose of demonstrating the usefulness of neutrinos. In the rare case that any of these scenarios would reflect an actual concern of the professional safeguards community, it is far from obvious that anyone in that community would want to admit it. Therefore, what is needed is a real-world case in which conventional methods did not yield the desired outcome for the IAEA and for which sufficient information is publicly available to perform a detailed technical analysis. The first North Korean nuclear crisis fits this bill on all accounts and we, therefore, have chosen it as our sandbox to explore the abilities and limitations of neutrino safeguards. Despite the brief discussion of the impact neutrino safeguards might have had on the unfolding of history in section 6.2, the main thrust of this study is not an attempt at counter-factual history but to demonstrate that under real-world constraints and boundary conditions, neutrino safeguards can provide a decisive advantage over conventional techniques, in particular, with a view of the next nuclear crisis in some other part of the world.

This paper is organized as follows: the technical aspects of neutrino safeguards and the

13. for a recent review on this topic, see Glenn R. Jocher et al., “Theoretical antineutrino detection, direction and ranging at long distances,” *Phys.Rept.* 527 (2013): 131–204, doi:10.1016/j.physrep.2013.01.005

14. Joel S. Wit, Daniel Poneman, and Robert L. Gallucci, *Going Critical: The First North Korean Nuclear Crisis* (Brookings Institution Press, 2007).

15. Zykov, “IAEA Instrumentation for the Future.”

general principles applicable to a wide range of reactor types and situations are presented in section 2 . In particular, figure 2 is one of our main results. In section 3, we present a summary of the first North Korean nuclear crisis based mostly on historic records. The specific features of the North Korean nuclear program relevant to this study are summarized in section 4. In section 5, we apply the techniques developed in section 2 to the particular problems posed by the North Korean nuclear program and provide detailed quantitative analysis for four detector deployment options. The resulting improvements in the quantitative understanding of the DPRK’s nuclear program and in particular the assessment of the veracity of the initial declaration of the DPRK to the IAEA are discussed in Sec 6. Also, a critical comparison to conventional techniques is offered. We summarize in section 7. Appendices A to C provide the details of our reactor simulations.

2 Antineutrino reactor safeguards

The fact that nuclear reactors are powerful neutrino sources was realized soon after nuclear reactors became practical. Neutrinos are not directly produced in nuclear fission but result from the subsequent beta-decays of the neutron-rich fission fragments. On average there are about 6 neutrinos per fission emitted and thus, for one gigawatt of thermal power a flux of about 10^{20} s^{-1} neutrinos is produced. The total number of emitted neutrinos is proportional to the total number of fissions in the reactor. Moreover, the distribution of fission fragments, and hence their beta-decays, are different for different fissile isotopes. Thus, careful neutrino spectroscopy should provide information not only on the total number of fissions but also about the fission fractions of the various fissile isotopes contained in the core. The basic concepts¹⁶ of both power monitoring and observing the plutonium content of a reactor were experimentally demonstrated in pioneering work performed by a group from the Kurchatov Institute lead by Mikaelyan. They deployed a neutrino detector of about 1 m^3 volume at the

16. Borovoi and Mikaelyan, “Possibilities of the practical use of neutrinos.”

Rovno nuclear power plant. For the power measurement, an agreement with the thermal measurements was found to within 2.5%¹⁷ and the effect due to a changing plutonium content was demonstrated;¹⁸ more recently the quantitative accuracy has been studied as well.¹⁹ This allows one to determine the plutonium content and power level of the reactor core *in situ* at a standoff distance of 10's of meters.²⁰ The practical feasibility of reactor monitoring using neutrinos has also been demonstrated using a small, tonne-size detector at the San Onofre power station, called SONGS.²¹

2.1 Neutrino detection

Beginning with the discovery of the neutrino, inverse beta-decay (IBD) has been the workhorse of reactor neutrino experiments

$$\bar{\nu}_e + p \rightarrow n + e^+ \quad (1)$$

In IBD, an electron antineutrino interacts with a proton to produce a neutron and a positron. Due to the mass difference of a neutron and a proton as well as the mass of the positron, this process has an approximate energy threshold of $(m_n - m_p + m_e)c^2 = 1.8 \text{ MeV}$. The positron will go on to annihilate with a nearby electron producing a pair of 511 keV gamma rays. This energy deposition is typically detected together with the kinetic energy of the positron E_e and thus the visible energy in detector, $E_{\text{vis}} = E_e + 2 \times 511 \text{ keV}$. There is a one-to-one correspondence between neutrino energy and the positron energy $E_\nu = E_e + 1.8 \text{ MeV}$. Here we neglect the recoil energy of the neutron which is much smaller than the energy resolution of even the best neutrino detectors. Therefore, a measurement of E_{vis} directly translates into

17. V. A. Korovkin et al., “Measuring Nuclear Plant Power Output by Neutrino detection,” *Soviet Atomic Energy* (1988): 712–718.

18. Yu. V. Klimov et al., “Measurement of variations of the cross section of the reaction $\bar{\nu}_e + p \rightarrow e^+ + n$ in the $\bar{\nu}_e$ flux from a reactor,” *Sov. J. Nucl. Phys.* 51, no. 2 (1990): 225–258.

19. Huber and Schwetz, “Precision spectroscopy with reactor anti-neutrinos.”

20. Yu. A. Klimov et al., “Neutrino method remote measurement of reactor power and power output,” *Atomic Energy* 76, no. 2 (1994): 123–127; Huber, “Spectral antineutrino signatures and plutonium content of reactors.”

21. A. Bernstein et al., “Monitoring the Thermal Power of Nuclear Reactors with a Prototype Cubic Meter Antineutrino Detector,” *J. Appl. Phys.* 103 (2008): 074905, doi:10.1063/1.2899178.

a measurement of the neutrino energy E_ν .

The reaction in equation 1 also results in a neutron, which in itself is invisible to the detector, but will slow down in collisions with the detector material and eventually undergo neutron capture. A careful choice of the nucleus on which the neutron captures allows tailoring this signature. Common neutron capture agents are gadolinium, e.g. Daya Bay²² or lithium, e.g. Bugey.²³ In the case of gadolinium, the signature of neutron capture is the emission of several gamma rays with a total energy of 8 MeV, whereas in the case of lithium the signature is the production of an alpha particle and a ^3H nucleus. The slowdown and capture of the neutron requires a characteristic time, allowing for what is called a delayed coincidence: there is a primary energy deposition from the positron followed somewhat later by a neutron capture signal. This delayed coincidence is key to separate neutrino events from backgrounds. The neutron capture cross sections of both gadolinium and lithium are much larger than of any of the other detector materials. Therefore, even small concentrations at a level of a percent or less will result in the majority of neutron captures occurring on those nuclei.

Eventually, all signatures will result in ionization and this ionization is detected by using organic scintillator which can be either liquid or solid. The organic nature of the scintillator provides the free protons for the interaction in equation 1. Recently, there have been three experiments²⁴ aimed at fundamental physics employing gadolinium-doped liquid scintillator at a large scale of several 10 tonnes without any safety incidents and excellent long-term stability. Specifically, throughout this paper we consider a 5 t detector based on organic scintillator corresponding to 4.3×10^{29} target protons. A real detector will not have 100% efficiency and to obtain the same number of events a larger detector will be needed. Many

22. F.P. An et al., “Observation of electron-antineutrino disappearance at Daya Bay,” *Phys.Rev.Lett.* 108 (2012): 171803, doi:10.1103/PhysRevLett.108.171803.

23. Y. Declais et al., “Search for neutrino oscillations at 15-meters, 40-meters, and 95-meters from a nuclear power reactor at Bugey,” *Nucl.Phys.* B434 (1995): 503–534, doi:10.1016/0550-3213(94)00513-E.

24. Y. Abe et al., “Indication for the disappearance of reactor electron antineutrinos in the Double Chooz experiment,” *Phys.Rev.Lett.* 108 (2012): 131801, doi:10.1103/PhysRevLett.108.131801; An et al., “Observation of electron-antineutrino disappearance at Daya Bay”; J.K. Ahn et al., “RENO: An Experiment for Neutrino Oscillation Parameter θ_{13} Using Reactor Neutrinos at Yonggwang” (2010).

neutrino detectors with efficiencies above 50% have been built and thus even a realistic detector yielding the same event numbers would be less than 10 t. A standard 20 feet intermodal shipping container has an interior volume of 33.1 m^3 and a net load capacity of 28.2 t, thus even a 10 t neutrino detector fits easily within such a container together with its support systems. The neutrino spectrum is divided in energy from 1.8 MeV to 8 MeV in bins of 0.2 MeV width, which at 4 MeV approximately corresponds to $10\%/\sqrt{E}$ resolution, which is similar to the resolution of recent experiments.²⁵ We checked that a resolution half as good would yield virtually identical results. For the IBD cross section we use the result of Vogel and Beacom²⁶ corrected for a neutron lifetime of 878.5 s ²⁷. For all measurements at reactors, the standoff is 20 m, which for both of the considered reactors would allow for deployment outside the reactor building. Such a detector at this standoff would typically register about 5,000 events per year for a reactor operating at 1 MW_{th} throughout that year.

2.2 Reactor flux models

More than 99% of the power in reactors, in a uranium fuel cycle, is produced in the fission of four isotopes: uranium-235, plutonium-239, uranium-238, and plutonium-241. A reactor with fresh fuel starts with only fissions in the uranium isotopes and plutonium is produced via neutron capture on uranium-238 as the burn-up increases. The total neutrino flux from a reactor ϕ can be written as

$$\phi(E) = \sum_I f_I S_I(E), \quad (2)$$

25. Abe et al., “Indication for the disappearance of reactor electron antineutrinos in the Double Chooz experiment”; An et al., “Observation of electron-antineutrino disappearance at Daya Bay”; Ahn et al., “RENO: An Experiment for Neutrino Oscillation Parameter θ_{13} Using Reactor Neutrinos at Yonggwang.”

26. P. Vogel and John F. Beacom, “Angular distribution of neutron inverse beta decay,” *Phys.Rev. D*60 (1999): 053003, doi:10.1103/PhysRevD.60.053003.

27. This values is taken from () and is very close to the value of 880 s currently recommended by the Particle Data Group,. () It should be mentioned that there still are measurements deviating significantly from that value by several standard deviations, see e.g.. ()

where f_I is the fission rate in isotope I and $S_I(E)$ is the neutrino yield for the isotope I . The thermal power of the reactor is also given in terms of the fission rates

$$P_{\text{th}} = \sum_I f_I p_I, \quad (3)$$

where p_I is the thermal energy release in one fission of the isotope I ; we use the values for p_I given by Kopeikin.²⁸ In order to be able to disentangle the contributions of the four isotopes, we need to know the neutrino yields S_I . These neutrino yields, in principle, are given by the neutrino spectra $\nu_k(E)$ of each fission fragment k and the cumulative fission yield for each fragment, Y_k^I ,

$$S_I(E) = \sum_k Y_k^I \nu_k(E), \quad (4)$$

where k typically runs over about 800 isotopes. In practice, we do not know the neutrino spectrum of a given fission fragment, but have only information regarding the beta spectrum and in many cases this knowledge is inaccurate, incomplete, or entirely missing. Even for a well known beta spectrum, significant complications arise from the conversion of a beta spectrum into a neutrino spectrum since each individual beta-decay branch has to be treated separately. As a result, a direct computation of the neutrino yields S_I via the summation of all individual neutrino spectra will be of limited accuracy,²⁹ but in many cases is the only available method.

A more accurate method is based on the measurement of the integral beta spectrum of all fission fragments³⁰ and subsequently the neutrino spectrum can be reconstructed from those

28. V. Kopeikin, L. Mikaelyan, and V. Sinev, “Reactor as a source of antineutrinos: Thermal fission energy,” *Phys.Atom.Nucl.* 67 (2004): 1892–1899, doi:10.1134/1.1811196.

29. Th. A. Mueller et al., “Improved predictions of reactor antineutrino spectra,” *Phys. Rev. C* 83, no. 5 (2011): 054615, doi:10.1103/PhysRevC.83.054615; M. Fallot et al., “New antineutrino energy spectra predictions from the summation of beta decay branches of the fission products,” *Phys.Rev.Lett.* 109 (2012): 202504, doi:10.1103/PhysRevLett.109.202504.

30. F. Von Feilitzsch, A.A. Hahn, and K. Schreckenbach, “Experimental beta spectra from Pu-239 and U-235 thermal neutron fission products and their correlated anti-neutrino spectra,” *Phys.Lett.* B118 (1982): 162–166, doi:10.1016/0370-2693(82)90622-0; K. Schreckenbach et al., “Determination of the anti-neutrino spectrum from U-235 thermal neutron fission products up to 9.5 MeV,” *Phys.Lett.* B160 (1985): 325–330, doi:10.1016/0370-2693(85)91337-1; A.A. Hahn et al., “Anti-neutrino spectra from Pu-241 and Pu-239

measurements.³¹ This method is less dependent on nuclear data about individual fission fragments but is not entirely free from uncertainties related to effects of nuclear structure.³²

We need to point out that the problem of neutrino yields has recently received significant scrutiny. Until the 2011 work by a group from Saclay,³³ the results by Schreckenbach et al.,³⁴ obtained in the 1980s at the Institut Laue-Langevin in Grenoble were considered the gold standard. The Saclay group, in preparation of the Double Chooz neutrino experiment,³⁵ revisited the previous results in an attempt to reduce the uncertainties. Instead, they found a upward shift of the central value of the average yield by about 3% while the error budget remained largely unchanged. This result, in turn, requires a reinterpretation of a large number of previous reactor neutrino experiments, since this changes the expected number of events. Together with the changes of the value of the neutron lifetime³⁶ and corrections from so-called non-equilibrium effects, the previous experiments appear to observe a deficit in neutrino count rate of about 6%; this is called the *reactor antineutrino anomaly* and was first discussed by Mention et al..³⁷ The initial result on the flux evaluation and the 3% upward shift was independently confirmed by one of the authors.³⁸ A plausible explanation could come in the form of a new particle, a sterile neutrino, which is not predicted by the Standard Model of particle physics. Given the far-flung consequences of the existence of this

thermal neutron fission products,” *Phys.Lett.* B218 (1989): 365–368, doi:10.1016/0370-2693(89)91598-0; N. Haag et al., “Experimental Determination of the Antineutrino Spectrum of the Fission Products of ^{238}U ” (2013).

31. Patrick Huber, “On the determination of anti-neutrino spectra from nuclear reactors,” *Phys.Rev.* C84 (2011): 024617, doi:10.1103/PhysRevC.85.029901, 10.1103/PhysRevC.84.024617.

32. Huber, “Anti-neutrino spectra”; A.C. Hayes et al., “Reanalysis of the Reactor Neutrino Anomaly” (2013).

33. Mueller et al., “Improved predictions.”

34. Von Feilitzsch, Hahn, and Schreckenbach, “Experimental beta spectra from Pu-239 and U-235 thermal neutron fission products and their correlated anti-neutrino spectra ”; Schreckenbach et al., “Determination of the anti-neutrino spectrum from U-235 thermal neutron fission products up to 9.5 MeV ”; Hahn et al., “Anti-neutrino spectra from Pu-241 and Pu-239 thermal neutron fission products .”

35. Abe et al., “Indication for the disappearance of reactor electron antineutrinos in the Double Chooz experiment.”

36. Fred E. Wietfeldt and Geoffrey L. Greene, “*Colloquium* : The neutron lifetime,” *Rev. Mod. Phys.* 83 (4 2011): 1173–1192.

37. G. Mention et al., “The Reactor Antineutrino Anomaly,” *Phys.Rev.* D83 (2011): 073006, doi:10.1103/PhysRevD.83.073006.

38. Huber, “Anti-neutrino spectra.”

sterile neutrino a considerable level of research activity ensued³⁹.

In table I the event rate predictions for various flux models are compared for the four fissile isotopes. The ENSDF flux model is based on thermal neutron fission yields of uranium-235, plutonium-239, and plutonium-241 from the JEFF database, version 3.1.1;⁴⁰ the fast neutron fission yield of uranium-238 from the ENDF-349 compilation conducted at Los Alamos National Laboratory;⁴¹ and on the beta-decay information contained in the Evaluated Nuclear Structure Data File (ENSDF) database, version VI.⁴² The neutrino spectrum is computed following the prescription of Huber.⁴³ Our ENSDF model represents a very crude summation calculation and we reproduce the measured total beta spectra⁴⁴ to within about 25%. A state-of-the-art summation calculation is given by Fallot *et al.*,⁴⁵ where great care is taken to replace the ENSDF entries with high quality experimental data where available and to use a carefully selected mix of databases. This model reproduces the measured total beta spectra⁴⁶ to within 10%. Finally, a direct deconvolution of the neutrino spectra from the total beta data was performed by Huber⁴⁷ for the isotopes uranium-235, plutonium-239, and plutonium-241, which to this date represents the most accurate neutrino yields for those isotopes. We note that the absolute values differ significantly between models, but once we normalize the predictions for total rate and mean energy to that of uranium-235, the predic-

39. for a recent review, see K.N. Abazajian et al., “Light Sterile Neutrinos: A White Paper” (2012)

40. “JEFF database,” <http://www.oecd-neo.org/dbdata/jeff/\#library>.

41. T. R. England and B.F. Rider, *ENDF-349 Evaluation and Compilation of Fission Product Yields: 1993*, LA-UR-94-3106, technical report (Los Alamos National Laboratory, 1994).

42. “ENSDF database,” <http://www.nndc.bnl.gov/ensdf/>.

43. Huber, “Anti-neutrino spectra.”

44. Von Feilitzsch, Hahn, and Schreckenbach, “Experimental beta spectra from Pu-239 and U-235 thermal neutron fission products and their correlated anti-neutrino spectra ”; Schreckenbach et al., “Determination of the anti-neutrino spectrum from U-235 thermal neutron fission products up to 9.5 MeV ”; Hahn et al., “Anti-neutrino spectra from Pu-241 and Pu-239 thermal neutron fission products ”; Haag et al., “Experimental Determination of the Antineutrino Spectrum of the Fission Products of ²³⁸U.”

45. Fallot et al., “New antineutrino energy spectra predictions from the summation of beta decay branches of the fission products.”

46. Von Feilitzsch, Hahn, and Schreckenbach, “Experimental beta spectra from Pu-239 and U-235 thermal neutron fission products and their correlated anti-neutrino spectra ”; Schreckenbach et al., “Determination of the anti-neutrino spectrum from U-235 thermal neutron fission products up to 9.5 MeV ”; Hahn et al., “Anti-neutrino spectra from Pu-241 and Pu-239 thermal neutron fission products ”; Haag et al., “Experimental Determination of the Antineutrino Spectrum of the Fission Products of ²³⁸U.”

47. Huber, “Anti-neutrino spectra.”

Table I: Rates and mean energies $\langle E \rangle$ for a 1 MW_{th} reactor in a 1 t detector at a standoff of 10 m measuring for 1 year for each individual isotope, assuming that only this isotope is fissioning. The three different flux models are explained in the text. Ratios are given relative to uranium-235.

	ENSDF			Fallot			Huber		
	rate ratio	$\langle E \rangle$ [MeV]	$\langle E \rangle$ ratio	ratio ratio	$\langle E \rangle$ [MeV]	$\langle E \rangle$ ratio	ratio ratio	$\langle E \rangle$ [MeV]	$\langle E \rangle$ ratio
uranium-235	1	4.48	1	1	4.28	1	1	4.25	1
uranium-238	1.53	4.59	1.024	1.56	4.45	1.040			
plutonium-239	0.64	4.26	0.950	0.65	4.13	0.965	0.66	4.04	0.951
plutonium-241	0.93	4.47	0.998	0.90	4.23	0.988	0.91	4.13	0.971

tions become very similar. In other words, the difference in neutrino yield and mean energy between the fissile isotopes is consistently predicted by the various flux models – which is not surprising given that these differences have their origin in the fission yields.

In practice, the current errors of any flux model are significant and a set of calibration measurements at reactors of known fissile content is likely required to mitigate the effect of these uncertainties, particularly in view of the reactor antineutrino anomaly. A proof of concept at a theoretical level for these calibrations has been performed.⁴⁸ On the experimental side, the Daya Bay collaboration has demonstrated the ability to cross-calibrate a set of 8 neutrino detectors to within better than 0.5%.⁴⁹

2.3 Reactor physics

The connection between fission rates and mass inventory requires a more detailed look at the reactor physics inside the core; our ultimate goal is to infer mass inventories. For a neutron flux which is constant in time and space, the fission rate and mass of a given fissile isotope have a simple linear relationship

$$f_I = \phi_n \sigma_I m_I, \quad (5)$$

48. Huber, “Spectral antineutrino signatures and plutonium content of reactors.”

49. F.P. An et al., “A side-by-side comparison of Daya Bay antineutrino detectors,” *Nucl.Instrum.Meth.* A685 (2012): 78–97, doi:10.1016/j.nima.2012.05.030.

where m_I is the mass of isotope I , σ_I is the energy averaged fission cross section and ϕ_n is the neutron flux. Throughout the evolution of the core, all factors on the right hand side of equation 5 will change. Due to burn-up effects, the mass m_I will change and the neutron flux typically will be adjusted to compensate for changes in reactivity while maintaining constant power. The accumulation of fission fragments will change the neutron absorption, which, in turn, alters the neutron energy spectrum; the cross section σ_I will evolve as well. The evolution of the isotopic content can be described by a set of Bateman equations and neutron transport methods can be used to recompute the relevant cross sections. We have performed evolution or burn-up calculations for several reactor types using the SCALE software suite.⁵⁰ For the further discussion it is useful to introduce fission fractions F_I , which are defined by

$$F_I = \frac{f_I}{\sum_I f_I} \quad \text{with} \quad \sum_I F_I = 1. \quad (6)$$

This definition has the advantage that the problem can be phrased independently of reactor power. For illustration, the time evolution of the F_I for a graphite moderated, natural uranium fueled reactor is given in the left hand panel of figure 1, where the fission fractions are shown as a function of the burn-up. F_{Pu241} is very close to zero in this type of reactor and therefore is not visible in this figure. The fission rate in uranium-238 stays constant since the amount of uranium-238 in the reactor changes very little with time. There is a clear anti-correlation between the fission fractions in uranium-235 and plutonium-239. The anti-correlation is nearly exact as shown in the right hand panel of figure 1 and we will make use of this later. In this context, it turns out that the burn-up is a useful variable which allows a summary of the reactor inventory with a single number. Burn-up measures the number of fissions which have occurred per unit of fuel mass or, in other terms, the amount of energy extracted; the unit for burn-up is MWd/t. For example, 1 tonne of fuel producing 5 MW for 1 day yields a burn-up of 5 MWd/t; the same burn-up would be obtained by 1 tonne of fuel

50. “SCALE,” <http://www.ornl.gov/sci/scale>.

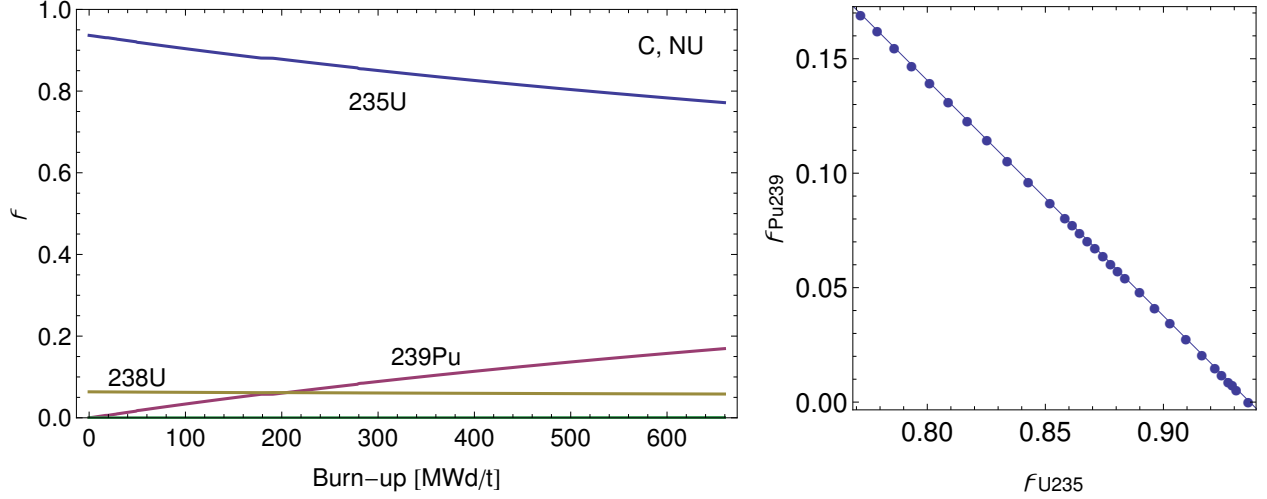


Figure 1: The left hand panel shows the evolution of the fission fractions in a graphite moderated natural uranium fueled reactor as a function of burn-up. The right hand panel shows the anti-correlation of the fission fractions in uranium-235 and plutonium-239.

running at 1 MW for 5 days. Neglecting radioactive decays, the isotopic composition of both samples would be identical since the total number of fissions which took place is the same. As a result, the reactor core evolution is, to a very high degree of accuracy, a function of only the burn-up. That is, details of the power history, like innage factors and shut downs, have only a minor impact on the reactivity and fission fractions. The amount of plutonium produced depends on the details of the reactor operations and so does the resulting neutrino signal. Therefore, we need to have a reasonably accurate model of the reactor power history, which in turn serves as input for a detailed reactor physics calculation. Neutrino emission is a result of radioactive decay of fission fragments and therefore, fuel of the same burn-up will have, to very good approximation, the same isotopic composition and will produce the same distribution and amount of neutrinos at a given power level. Therefore, our ability to predict the neutrino emission over time relies on an accurate model of the burn-up as a function of time.

This burn-up calculation also allows for the study of the time evolving relation between fission fractions and mass inventory as given in equation 5. We find, to very good accuracy, this is a linear relationship and the time evolution of the proportionality constant $\phi_n \sigma_I$,

throughout the fuel cycle, is very small. Using a fixed value for $\phi_n \sigma_{\text{Pu239}}$, throughout the reactor cycle, induces a root mean square error of 2% for plutonium mass determinations for a graphite moderated reactor and errors of similar size for the other reactor types considered later. This type of sensitivity study needs to be performed for each reactor type and design. Also, the actual values of $\phi_n \sigma_I$ have to be determined for each specific case.

2.4 Plutonium content determination

The difference in the spectral neutrino yield, of the four fissile isotopes, can be used to disentangle the contribution of each of those isotopes to the total neutrino flux. In order to do so, we set up a binned χ^2 -analysis, where the event rate in each bin n_i is given as

$$n_i = N \sum_I f_I \int_{E_i - \Delta E/2}^{E_i + \Delta E/2} dE \sigma(E) S_I(E), \quad (7)$$

where E_i is central energy of bin i , ΔE is the bin width and $\sigma(E)$ is the IBD cross section. N is an overall normalization constant set by the detector mass, or number of free protons, detection efficiency, and time interval of data taking. In order to compute the event rates n_i , we have to specify the four fission rates $\mathbf{f} = (f_{\text{U235}}, f_{\text{U238}}, f_{\text{Pu239}}, f_{\text{Pu241}})$. We denote the true or input values for our calculation by a superscript 0, i.e. the true fission rates are \mathbf{f}^0 and, in the same way, we will denote the n_i computed for the true values \mathbf{f}^0 as n_i^0 . We define the χ^2 -function as

$$\chi^2(\mathbf{f}) := \sum_i \frac{(n_i(\mathbf{f}) - n_i^0)^2}{n_i^0}, \quad (8)$$

This χ^2 -function will be zero for $\mathbf{f} = \mathbf{f}^0$. The allowed region for \mathbf{f} is obtained by requiring that

$$\chi^2(\mathbf{f}) \leq \chi_c^2, \quad (9)$$

where the critical value χ_c^2 is determined from a χ^2 probability distribution with, in this case, 4 degrees of freedom. If we are only interested in the total number of fissions in plutonium

given by $f_{\text{Pu}} = f_{\text{Pu239}} + f_{\text{Pu241}}$, the following marginalized function has to be used

$$\bar{\chi}^2(f_{\text{Pu}}) = \min_{f_{\text{U235}}, f_{\text{U238}}, \kappa} \chi^2(f_{\text{U235}}, f_{\text{U238}}, (1 - \kappa)f_{\text{Pu}}, \kappa f_{\text{Pu}}), \quad (10)$$

and in this case, since we are interested only in the single parameter f_{Pu} the number of degrees of freedom is 1. Similarly, we can define a corresponding single parameter function for the measurement of reactor power.

To relate a measured value of f_{Pu} to the mass inventory, a reactor physics simulation is required. f_{Pu} will be proportional to the plutonium mass, m_{Pu} , in the reactor

$$\gamma = \frac{m_{\text{Pu}}}{f_{\text{Pu}}}, \quad (11)$$

where γ is the proportionality constant. Therefore, a measurement of f_{Pu} translates into a determination of m_{Pu} . γ , in turn, depends on the details of the reactor physics as well as the instantaneous reactor thermal power; note that according to equation 5, $\gamma = 1/(\phi_n \sigma_{\text{Pu}})$ and thus is inverse to the neutron flux density ϕ_n . The determination of m_{Pu} and its connection to γ is clearly illustrated in figure 2, where we show the accuracy in the determination of m_{Pu} for a variety of reactor types as a function of the thermal power. This figure is based on a full calculation of the reactor burn-up, where “C, NU” corresponds to a graphite moderated reactor running on natural uranium and the dot on this line is the 5 MW_e reactor, whose simulation details are explained in appendix A. “H₂O, HEU” and “H₂O, HEU + NU” correspond to the IRT with drivers only and to the IRT with drivers and targets, respectively. The details of the simulation are explained in appendix. C. The case “H₂O, LEU” is computed for a typical pressurized light water reactor. We have taken a power history from one such reactor, with a total fuel load of 72.4 MTU⁵¹ enriched to 3.7%. The case “D₂O, NU” describes a heavy water moderated reactor running on natural uranium modeled on a CANDU design

⁵¹. MTU stands for metric tonne of uranium and is often synonymous with metric tonnes of heavy metal (HM), where heavy refers to all actinides including plutonium.

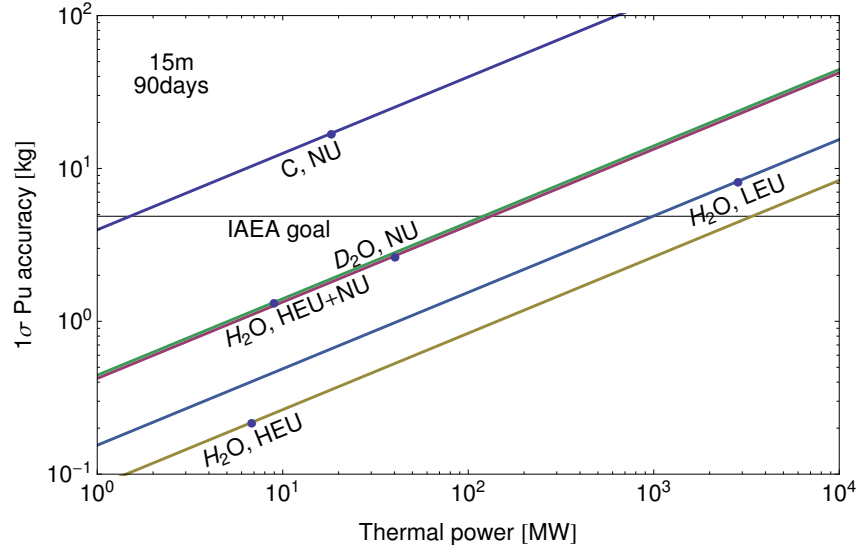


Figure 2: Absolute accuracy in the determination of the plutonium content based on the measurement of the neutrino spectrum as a function of the thermal power of the reactor. The different lines stand for different types of reactors as indicated by the labels: the first term indicates the type of moderator, whereas the second part denotes the fuel type, natural uranium (NU), low enriched uranium (LEU) and highly enriched uranium (HEU). This figure assumes a 5 t detector, a standoff of 15 m from the reactor core, and 90 days of data taking. The horizontal line labeled “IAEA goal” indicates the accuracy which corresponds to the detection of 8 kg of plutonium at 90% confidence level.

with a 8.6 MTU natural uranium fuel load and running at 40 MW_{th}. The 40 MW_{th} point on this line resembles, in many aspects, the Iranian reactor at Arak⁵² and the accuracy would be at the level of 2.7 kg within 90 days. The details of the calculations for the “H₂O, LEU” and “D₂O, NU” can be found in appendix B. The horizontal line corresponds to a sensitivity to 8 kg plutonium within 90 days, which is the stated IAEA goal⁵³.

For all of those quite different reactor types the accuracy of a m_{Pu} measurement can be described by the following simple relation

$$\delta m_{\text{Pu}} = 1.942 \text{ kg} \left(\frac{\gamma}{10^{-16} \text{ kg s}} \right) \left(\frac{L}{\text{m}} \right) \left(\frac{P_{th}}{\text{MW}} \right)^{1/2} \left(\frac{\text{tonnes}}{M} \right)^{1/2} \left(\frac{\text{days}}{t} \right)^{1/2}, \quad (12)$$

52. David Albright and Christina Walrond, *Update on the Arak Reactor*, technical report (Institute for Science and International Security (ISIS), 2013).

53. The IAEA uses this interpretation of the term significant quantity as the design basis for planning routine inspections in declared facilities. Any amount of fissile material diversion, or undeclared production, would be sufficient to warrant suspicion and follow-up activities to determine whether or not non-compliance might be considered by the IAEA Board of Governors.

where L is the standoff of the neutrino detector, P_{th} is the average thermal reactor power, M is the detector mass in tonnes (assuming 8.65×10^{28} protons per tonne), and t is the length of the data taking period. Table II lists the corresponding values of γ , and using those values,

Table II: The values of γ for a number of reactor types.

reactor type	C, NU	H ₂ O, HEU	H ₂ O, HEU+NU	D ₂ O, NU	H ₂ O, LEU
$\gamma [10^{16} \text{ kg s}]$	2.889	0.064	0.337	0.299	0.108

equation 12 reproduces the results of the full calculation within a few percent. For graphite moderated reactors, we find that the resulting δm_{Pu} is significantly larger, by a factor of at least 8.5, than for any other reactor type we have investigated. As we will show in the following, the fact that neutrino safeguards still yield meaningful results and are applicable for this reactor type is a testimony to the great versatility and power of this technique.

For most reactor running conditions, the variation in γ is very small and depends only very weakly, at the level of a few percent, on burn-up and reactor history. This implies that our result most likely will hold up even for detailed 3-dimensional reactor physics calculations, taking into account spatial burn-up variations.

We further observe, that for reactors with a thermal power in excess of 1 GW_{th} , which is the bulk of all reactors globally used for electricity production, this approach to safeguards will have difficulties in meeting the IAEA goal of detection of 1 significant quantity, which for plutonium is 8 kg, within 90 days⁵⁴. On the other hand, neutrino safeguards is quite straightforward for research, small modular reactors, and plutonium production reactors.

As discussed in the previous section, the fission fractions and thus the fission rates are *not* independent from each other but are coupled by the physics inside the reactor; for an illustration, see the right hand panel of figure 1. In trying to determine the plutonium mass inventory, we can make use of these correlations. Basically, reactor physics determines how the fission rates evolve together with burn-up. Therefore, a reactor model will provide the

⁵⁴. Plutonium in irradiated fuel is a so-called *indirect use nuclear material* and the precise IAEA goal is a 90% or higher confidence level detection of the diversion of 1 significant quantity within 90 days, according to International Atomic Energy Agency, *IAEA safeguards glossary* (International Atomic Energy Agency, 2002).

fission rates as a function of burn-up. This allows a rephrasing of the fitting problem in terms of one independent quantity – the burn-up. The result of the analysis will be a value for burn-up and some error bounds and since the reactor model also provides all the mass inventories as a function of burn-up, a measurement of the burn-up translates into a measurement of the core inventory and the errors can be determined by standard error propagation. In the case of the graphite moderated reactor this reduces the error in plutonium mass determination by roughly 50%; for details, see section 5.1. One potential drawback is the reliance on a reasonably accurate reactor model. In cases where there is reliable design information and the key operating parameters are known the burn-up model will reproduce the core inventory to within the 5-10% range, which for most purposes will be a small extra contribution to the overall error budget. In those cases, where the reactor design and operating parameters have to be considered as unknown or the knowledge is deemed unreliable, a fit to fission fractions and power should be performed. The loss in sensitivity is moderate compared to the increase in reliability of the result.

3 Summary of the 1994 crisis

The DPRK is rather unique in many regards, including its use of a nuclear weapons program as a bargaining tool. The direct tactical use of its small and crude nuclear arsenal against the U.S., or its regional allies like South Korea or Japan, is presumably deterred by the threat of U.S. retaliation. It is a serious concern that North Korea may share its nuclear know-how, materials, or even a fully functional weapon with third parties, but the fear of the likely attribution in case of a nuclear incident and the accompanying U.S. reaction may counteract this risk.⁵⁵ So far, North Korea obtained the largest benefit from its nuclear adventures by offering to abstain in the future. For the use as a bargaining tool, it is desirable to create a large degree of ambiguity about the type and scope of nuclear activities. At the same time,

⁵⁵ Siegfried S. Hecker and William Liou, “Dangerous Dealings: North Korea’s Nuclear Capabilities and the Threat of Export to Iran,” *Arms Control Today* (2007).

there are indications that North Korea was surprised by the level of information IAEA could glean from environmental sampling and allowing the IAEA to employ this method in the initial inspections may have been a serious miscalculation on the side of North Korea.⁵⁶ The three nuclear tests in 2006, 2009, and 2013 have removed a great deal of ambiguity about the kind and goal of North Korea's nuclear activities, but they shed no light on the scope of activities and the size of the resulting arsenal. New concerns have surfaced relating to the uranium enrichment program.⁵⁷

The DPRK signed the NPT on December 12, 1985; a safeguards agreement entered into force on April 10, 1994; and notice of withdrawal from the treaty was given on January 10, 2003.⁵⁸ On February 26, 1993, the IAEA called for special inspections, which in retrospect may have been counterproductive,⁵⁹ to resolve the discrepancies found during the first safeguards inspections in 1992. The issue of contention was the amount of plutonium the DPRK had separated from spent nuclear fuel – North Korea declared it produced about 90 g,⁶⁰ but IAEA data allowed for the possibility of a much larger amount, maybe as much as 14 kg,⁶¹ which would be sufficient to build two or more nuclear bombs. On March 12, 1993, the DPRK declared its intention to leave the NPT by June 12, 1993 after being threatened with special inspections but was persuaded by the U.S. on June 11 not to do so. A detailed representation of the time line is given in figure 3.

IAEA safeguards ended in 2003 and therefore we would like to focus on the time before 2003. Would antineutrino reactor safeguards have been able to reduce the pre-2003 ambiguities about the DPRK's plutonium production program and what would the potential impact of this information on the development of the crisis have been?

56. Mohamed ElBaradei, *The Age of Deception: Nuclear Diplomacy in Treacherous Times* (Metropolitan Books, 2011).

57. Siegfried Hecker, "A Return Trip to North Korea's Yongbyon Nuclear Complex" (Center for International Security and Cooperation, Stanford University, 2010).

58. David Fischer, *History of the International Atomic Energy Agency : the first forty years* (The Agency, 1997).

59. ElBaradei, *Age of Deception*.

60. Don Oberdorfer, *The two Koreas: a contemporary history* (Basic Books, 2001), p. 269.

61. David Albright, "How much plutonium does North Korea have?" *Bulletin of the Atomic Scientists* 50, no. 5 (1994): 46.

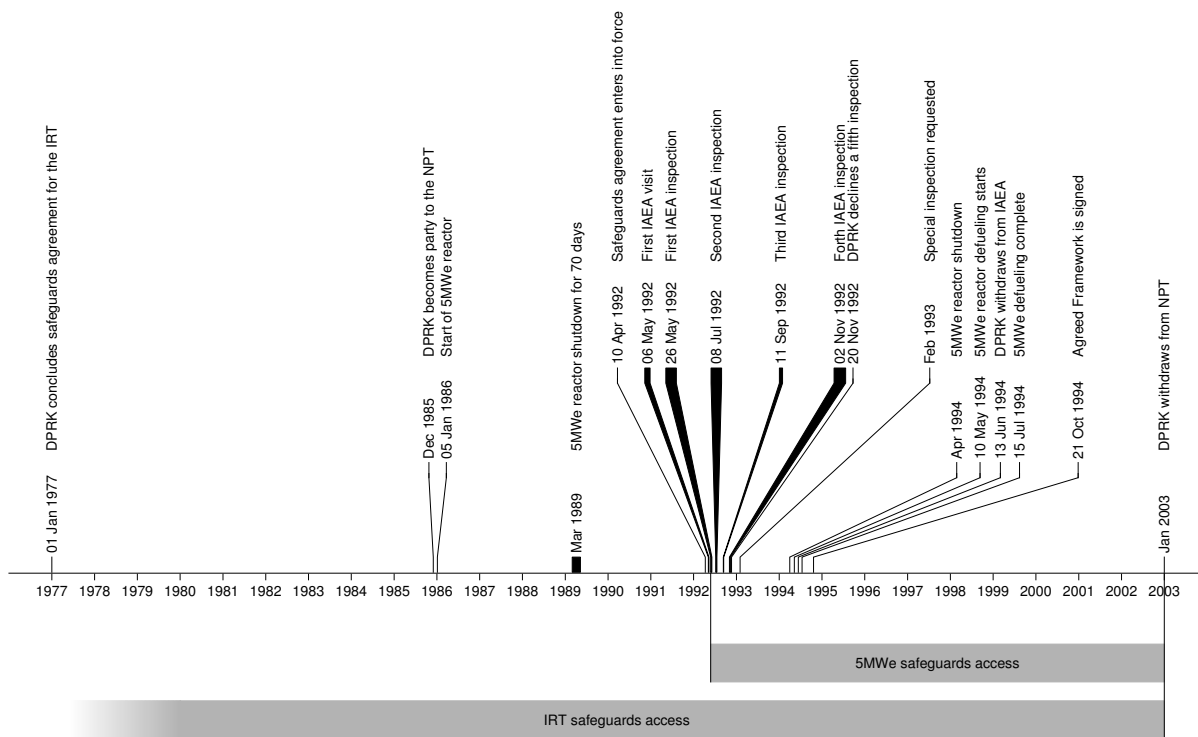


Figure 3: Time line of events

North Korea joined the NPT in 1985, but it took until spring of 1992 for a safeguards agreement to enter into force. North Korea started its 5 MW_e reactor at Yongbyon in 1986. In 1989 there was a 70 day shutdown, providing an opportunity to unload between 50-100% of the spent fuel in the core. In its initial declaration to IAEA in 1992, North Korea indicated that they ran a one-time reprocessing campaign in 1990 that resulted in 90 g of plutonium from a limited number of damaged fuel rods removed during the 1989 shutdown. The results of IAEA environmental sampling conducted during the first safeguards inspection in 1992, however, indicated at least three campaigns of reprocessing in 1989, 1990, and 1991⁶² which in turn admits the hypothesis that a significant fraction of the spent fuel had been removed in 1989 and subsequently reprocessed. As a result, a larger amount of separated plutonium may have been obtained by the DPRK, possibly sufficiently large to build two or more nuclear bombs. Given the ramifications of these findings, IAEA Director General Hans Blix insisted on a definitive resolution of this question as a precondition to declare the DPRK to be in compliance with its commitments under the NPT. In particular, finding and sampling the reprocessing waste streams was a priority for IAEA, eventually triggering the request for special inspections.⁶³ The diplomatic exchange between IAEA and the DPRK dragged on in parallel with negotiations between the DPRK and the U.S.; the latter eventually leading to the Agreed Framework. In April 1994 North Korea forced the issue by beginning to unload spent fuel from the reactor core. An analysis of the gamma-radiation of spent fuel taken at known positions in the reactor core would have resolved the question of how much spent fuel was discharged in 1989 and whether the North Korean declaration was correct. Knowing the original position of a sample in the reactor core is crucial for this analysis, since the fission rate is higher in the center than at the edge of the core; for technical details of this method see section 6.1. However, the unloading proceeded very fast and it appears as if the operators took deliberate steps to obliterate any information about the original position of each fuel element in the reactor; effectively, IAEA inspectors could only observe the unloading but

62. Albright, "How much plutonium does North Korea have?"

63. O. Heinonen, Interview by PH, April 16 2013.

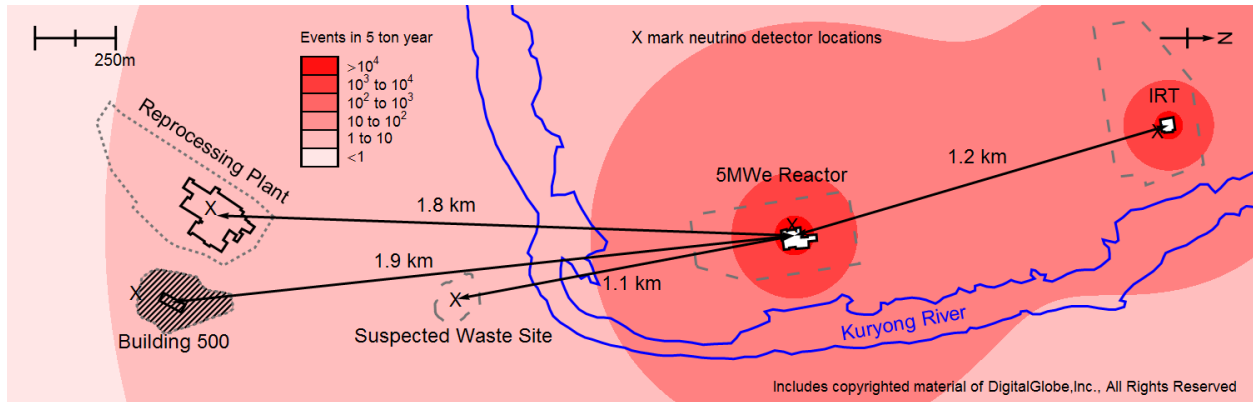


Figure 4: A map of relevant boundaries and geographies of the Yongbyon nuclear facility. Contours show expected inverse beta-decay event rates for a 5 t detector over the course of a year. X's mark the location of various neutrino detectors used in the paper. The satellite image on which this map is based was taken on May 16, 2013 by GeoEye-1.

were unable to take any meaningful measurements of any individual fuel elements as they were being removed, or to make a connection between the fuel elements and the core locations they had occupied. As a result, crucial evidence was denied to the IAEA and on June 2, 1992 Blix declared that the ability to resolve the issue had been “seriously eroded”.⁶⁴ The fuel discharged in 1994 was canned using U.S. equipment and subsequently was put into storage and was under IAEA surveillance until 2003, when the DPRK declared its withdrawal from the NPT. The 1994 crisis was resolved by the so called *Agreed Framework* under which the DPRK halted any plutonium production and fuel reprocessing in exchange for the promise to obtain two pressurized light-water reactors at not cost.⁶⁵ The *Agreed Framework* unraveled in 2003 and eventually, in 2006, North Korea conducted its first nuclear test explosion.

4 Plutonium production in the DPRK

A comprehensive account of the history of the North Korean nuclear program is provided by Hecker.⁶⁶ For our purposes, three facilities are relevant: a Soviet supplied research reactor

64. Albright, “How much plutonium does North Korea have?”

65. Wit, Poneman, and Gallucci, *Going Critical*.

66. Hecker and Liou, “Dangerous Dealings”; Siegfried Hecker, “Lessons learned from the North Korean nuclear crises,” *Dædalus* Winter (2010): 44–56.

with a power of around 8 MW_{th} , the IRT; a graphite moderated reactor with a thermal power of approximately $20 \text{ MW}_{\text{th}}$, which generally is referred to by its electrical power, hence the name 5 MW_{e} ; and the Radiochemical Laboratory, which is a reprocessing facility which allows for the extraction of plutonium from the spent fuel from the 5 MW_{e} reactor. These facilities and their relative locations are shown in figure 4. Features such as the river and relevant buildings are outlined, neutrino detector locations are marked, and IBD event rate iso-contours are shown.

In the 1960s, the IRT was supplied by the Soviet Union.⁶⁷ This reactor is a light-water moderated reactor running on highly enriched uranium, with enrichment from 10% to 80%⁶⁸. The Soviet Union also provided the HEU fuel until its own demise in the 1990s. With this reactor, the Isotope Production Laboratory, a facility for handling irradiated materials, was provided. The nominal power of this reactor is 8 MW_{th} . Using the laboratory, early, small scale plutonium separation experiments may have been conducted with fuel or targets irradiated in this reactor.⁶⁹

North Korea started serious fuel cycle activities in the 1980s and the plan was to build and operate three gas-cooled, graphite moderated, natural uranium fueled reactors. A 5 MW_{e} and 50 MW_{e} reactor were foreseen for the Yongbyon site and a $200 \text{ MW}_{\text{e}}$ power reactor was planned at Taechon. The design followed the British Magnox design, where Magnox is the name of the alloy used for the fuel cladding: magnesium non-oxidizing. The thermal power of Magnox reactors is typically 4-6 times higher than the above quoted electrical power, so they are much less efficient than, for instance, pressurized light-water reactors, where this factor is closer to 3. Apart from efficiency, the choice of Magnox has another severe drawback: Magnox fuel cladding corrodes in contact with water such that long term storage of spent fuel under water is not possible. This makes encapsulation or some level of reprocessing

67. Hecker, "Lessons learned."

68. David Albright and Kevin O'Neill, eds., *Solving the North Korean Nuclear Puzzle* (ISIS Press, 2000), p. 148.

69. Ibid., p. 92.

essentially mandatory.⁷⁰ The attractive features of this design are its simplicity and that it does not require uranium enrichment or the use of exotic moderators like heavy water. So, this reactor type was well adapted to North Korean indigenous industrial capabilities. At the same time, Magnox reactors were originally designed as dual-use facilities to produce both electricity *and* weapons-grade plutonium.

The amount of plutonium produced in a reactor can be estimated if the integrated neutron flux, which is proportional to the total energy produced, is known, or equivalently if a *complete* history of the reactor power is available. It turns out that all uncertainty about the produced amounts of plutonium center on the issue of the completeness, and to a lesser degree, the uncertainty of the record of the power history. To obtain the produced plutonium in usable form, the reactor has to be shut down⁷¹, the irradiated fuel rods removed, and the plutonium then needs to be chemically separated from the spent fuel at the Radiochemical Laboratory. The location of the various facilities can be seen in figure 4.

The time evolution of the burn-up for the 5 MW_e is shown in figure 5 which has been adapted from *Nuclear Puzzle* and is deemed accurate.⁷² The information in this figure is the backbone of the analysis presented here and our quantitative results are based on this information. The blue curve is based on the declarations made by the DPRK and, thus, the assumption is that no major refueling has taken place in 1989. The orange curve is derived assuming that the full core has been replaced with fresh fuel in 1989 under the constraint of arriving at the same final burn-up. These numbers can be readily converted into reactor thermal power levels using the fact that there are approximately 50 tonnes of uranium in this reactor.⁷³ The power levels then form the input for a detailed calculation of the reactor isotopic composition and fission rates for the various fissile isotopes. The software we used

70. Albright, “How much plutonium does North Korea have?”

71. In principle, Magnox reactors can be refueled under load, but the DPRK seems not to have mastered this technology at that time.

72. O. Heinonen, Interview by PH, April 16 2013, Heinonen confirms, looking at fig. VI.2 of *Nuclear Puzzle* that this is an accurate description of the burn-up.

73. Albright and O’Neill, *Nuclear Puzzle*.

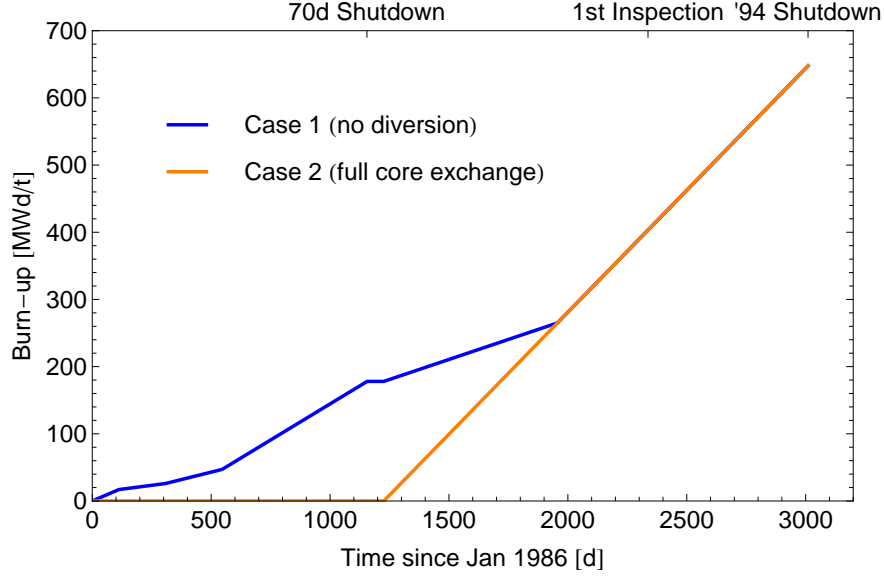


Figure 5: Burn-up of the fuel in the 5 MW_e reactor as function of time measured in days since January 1, 1986. The blue curve is based on the values declared by the DPRK, i.e. no major refueling has taken place in 1989. The orange curve is derived assuming that the full core has been replaced with fresh fuel in 1989. Figure adapted from Albright and O'Neill, *Nuclear Puzzle*.

to compute the relevant reactor parameters is called SCALE⁷⁴ and is considered a standard method for this type of problem. The details of the calculation can be found in appendix A.

5 Neutrinos in the DPRK case

The basic analysis techniques developed in the previous section can now be applied to the specific situation in the DPRK in the time frame of 1986-1994. The central question for the international community, after the initial discrepancies appeared in 1992, was how much plutonium the DPRK had separated. The lower bound on this quantity is represented by assuming that the DPRK's initial declaration to IAEA was quantitatively correct, i.e. only 90 g of plutonium were separated from a few hundred damaged fuel elements discharged and replaced during the 1989 shutdown. The upper bound on the amount of separated plutonium is obtained by assuming that the full core with a burn-up of approximately 200 MWd/t was discharged in 1989, containing 8.8 kg of plutonium and that this full core was subsequently

⁷⁴. "SCALE."

reprocessed. The North Korean scientists could have produced additional plutonium over a long period of time by irradiating natural uranium targets in the IRT, resulting in roughly 0.5 kg of plutonium per 250 day run of the IRT. The limited amount of Soviet supplied fuel and the fact that the IRT was under IAEA safeguards from 1977 on limits the amount the DPRK could have produced via that route to less than 1 kg.⁷⁵ Other authors⁷⁶ estimate the theoretical upper limit of the amount of plutonium to be as large as 4 kg.

As far as the 5 MW_e reactor is concerned, at the time of the first IAEA inspection in 1992, the burn-up and reactor power were the same for both the extreme cases (see figure 5). Therefore, our analysis will include the hypothetical scenario where neutrino safeguards were applied before and after the 1989 shutdown⁷⁷. The specific unique capability represented by neutrino safeguards in this case derives from the ability to measure the power history and burn-up *independently* – any mismatch indicates a fuel diversion.

In the PUREX process for reprocessing, the fission fragments remain in the aqueous phase and therefore will end up in the waste. Some of these fission fragments produce neutrinos above IBD threshold even after a considerable time interval has elapsed, which we will refer to as long-lived isotopes (LLI), in particular: strontium-90 with a half-life of 28.9 y, ruthenium-106 with a half-life of 372 d, and cerium-144 with a half-life of 285 d. These three isotopes have large direct fission yields and are produced in amounts which are proportional to the number of total fissions and thus are accurate tracers of burn-up. Detecting neutrinos from LLI is a direct method to find reprocessing wastes and, in principle, also yields an estimate of the amount of plutonium separated. Given the high penetrating power of neutrinos, this method is equally applicable to buried wastes.

Finally, neutrinos can travel arbitrary distances, and thus a neutrino detector deployed

75. O. Heinonen, Interview by PH, April 16 2013, Heinonen estimates that the upper limit is between 0.5-1 kg, based on the detailed fuel burn-up data the IAEA obtained as part of its safeguards agreement for the IRT.

76. Albright and O'Neill, *Nuclear Puzzle*, p. 120.

77. In principle, the amounts of the long-lived isotopes strontium-90, ruthenium-106, and cerium-144 will be different between the two irradiation histories which leads to differences in the low energy neutrino spectrum below 3.6 MeV. However, extensive calculations show that the resulting event rate differences in 1992 are too small to be reliably detected.

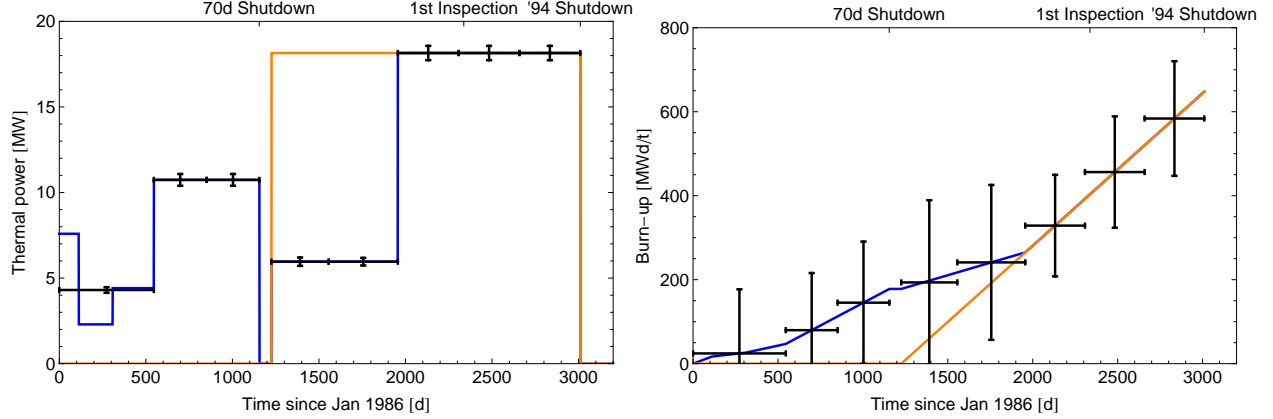


Figure 6: In the left hand panel, 1σ sensitivities to reactor power are shown for varying data collection periods using a 5 t detector at 20 m standoff from the 5 MW_e reactor. Fission fractions are free parameters in the fit. In the right hand panel, 1σ sensitivities to burn-up are shown, where power is a free parameter in the fit. The blue curve shows the history under the assumption of no diversion. The orange curve shows history for the case of a full core discharge in 1989.

for safeguarding the IRT would also be sensitive to neutrinos from the 5 MW_e , especially during times when the IRT is shut down. This signal will allow a remote power measurement which can distinguish the two cases shown in figure 5.

5.1 5 MW_e reactor

In the following analysis, sensitivities to power, burn-up, and plutonium content are determined based on the declared power history. This history is displayed as blue curves in the various figures in this section. Comparisons are made to a hypothetical undeclared core swap to a fresh reactor core during the 70 day shutdown period, displayed as orange curves. The difficulty in determining the difference between the two curves lies in the fact that after 1992, power and burn-up are the same. As seen in figure 11, after the 1st inspection, all the fission rates from the four primary fissioning isotopes are identical with or without diversion. For the following analyses, a standard 5 t detector at 20 m standoff from the reactor is used, which for a data taking period of one year corresponds to about 95,000 events.

A power sensitivity computation is first considered. The analysis is done using the

following χ^2 -function

$$\chi^2 = \sum_i \frac{1}{n_i^0} \cdot \left[\left(N P_{\text{th}} \sum_I F_I S_{I,i} \right) - n_i^0 \right]^2, \quad (13)$$

where F_I is the fission fraction for isotope I , n_i^0 is the measured number of neutrino events in energy bin i , and $S_{I,i}$ is the neutrino yield in energy bin i for isotope I . P_{th} is the thermal power and N is a normalization constant. Moreover, the fission fractions F_I are subject to a normalization constraint as given in equation 6.

The resulting 1σ sensitivities are shown in the left hand panel of figure 6. This analysis assumes precise knowledge of the distance from the reactor to the detector and treats them both as points. Any uncertainty in the geometric acceptance will directly relate into an uncertainty of the normalization constant, N , and thus into an uncertainty in the power P_{th} . Neglecting this potential source of systematic uncertainty, a power accuracy of around 2% can be achieved.

A similar analysis can be done to determine the sensitivities for burn-up, BU , using equation 13. In this circumstance, P_{th} is free in the fit and the fission fractions F_I are now functions of burn-up, determined by a reactor core simulation as described in appendix A. The results of this analysis are shown in the left hand panel of figure 6. Burn-up across the history of the reactor has an error of $\sim 100 \text{ MWd/t}$. Closely related to the burn-up is the amount of plutonium in the nuclear reactor. This analysis is done again using equation 13. This time, P_{th} as well as $F_{\text{U}235}$ and $F_{\text{U}238}$ are free parameters as well as the relative contribution of the two plutonium fission rates, κ , and the resulting sensitivities are shown as dashed black lines in figure 7. Alternatively, one can use the burn-up sensitivity to constrain the plutonium content as well. After computing burn-up errors, a reactor model is used to compute the change in plutonium fissions. This is shown as the solid black error bars. These errors are given both in terms of raw plutonium fissions in the left hand panel as well as the corresponding plutonium masses in the right hand panel. In the right hand

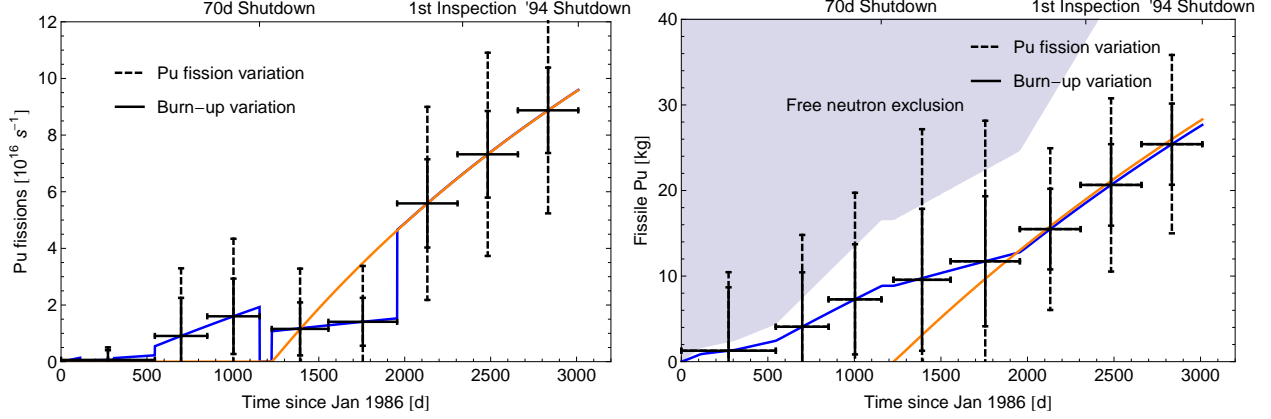


Figure 7: 1σ sensitivities to plutonium are shown for varying data collection periods using a 5 t detector at 20 m standoff from the 5 MW_e reactor. The blue curve shows the plutonium-239 history under the assumption of no diversion. The orange curve shows the plutonium-239 history if there had been diversion. Black dashed error bars show the 1σ sensitivity by measuring the plutonium fission rates with uranium fission rates and reactor power free in the fit. Solid black error bars show the 1σ sensitivity determined by constraining the burn-up using a reactor model. The left plot shows the errors on absolute plutonium fission rates and the right plot show the corresponding errors for plutonium mass with a shaded exclusion region from the assumption that all neutrons not needed for fission are available for the production of plutonium.

panel, a very naive exclusion region is shown for comparison. It assumes that each of the 1.7 neutrons per fission not being used to sustain the chain reaction is instead available to produce more plutonium. This limit is shown as the shaded region in the right hand plot.

5.2 IRT reactor

The IRT is assumed to run for a 250 day period followed by a 100 day shutdown,⁷⁸ and the fission rates are computed in appendix C and shown in figure 12. The natural uranium targets provide much more uranium-238, changing the fission fractions substantially and allowing an order of magnitude increase in plutonium-239 production and fissions. As with the 5 MW_e reactor, it is assumed that a 5 t neutrino detector is placed 20 m away from this reactor. The χ^2 from equation 13 can be used to determine the thermal power to within 0.6 MW in each 50 day period. All other things the same, the addition of targets will increase the power output of the reactor. As long as the detector distance and mass were sufficiently

78. Albright and O'Neill, *Nuclear Puzzle*, pp.148-165.

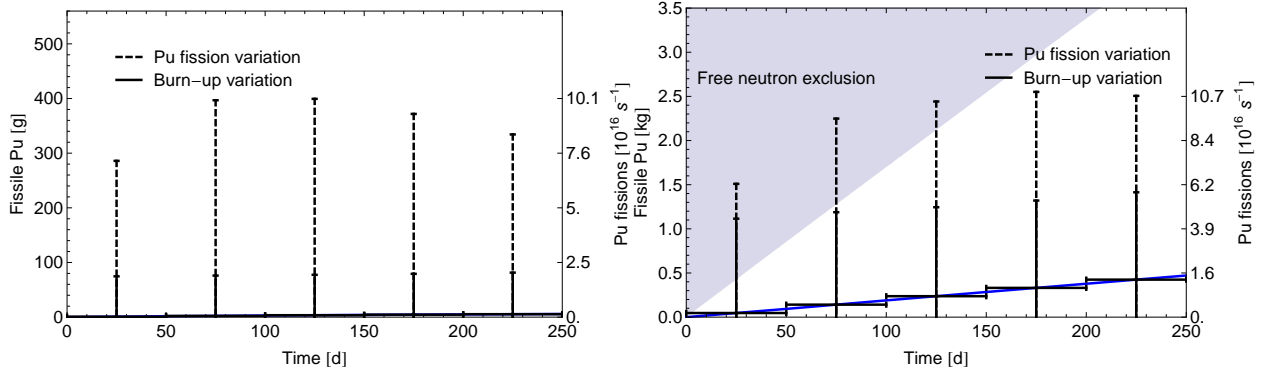


Figure 8: 1σ sensitivities to reactor plutonium fissions are shown for 50 day collection periods using a 5 t detector, 20 m away from the IRT reactor. Black dashed error bars show the 1σ sensitivity resulting from measuring the plutonium fission rate with uranium contributions and power free in the fit. The solid black error bars show the 1σ sensitivity determined using a burn-up model. The left plot shows driver only results and the right plot shows results for driver and targets combined.

well known, the errors would be small enough to clearly notice the power difference caused by the addition of breeding targets. At the same time, it would be trivial for the operator to adjust the power with targets to remain the same as without targets, which would reduce plutonium production by about 25%.

The 1σ errors on plutonium content can be determined by measuring the fission rates using the χ^2 prescription in equation 13 and then converting these to a plutonium mass using equation 5. Alternatively, one can determine the burn-up in conjunction with a reactor model and then infer the errors on plutonium mass inventory. The results of the analysis are shown in figure 8. Similar error bars are found on raw plutonium fission rates, with and without the targets. Note, that these are also similar to the 5 MW_e reactor results. Very different, however, are the sensitivities to the mass of plutonium. In the case with only drivers, a neutrino detector would be sensitive to tens of grams of plutonium. With both the drivers and targets, there is an order of magnitude increase in the errors into the hundreds of grams of plutonium. The difference is even more pronounced in comparison to the 5 MW_e reactor, where plutonium mass sensitivities in the multi-kg range are obtained. Despite similar sensitivities for plutonium fission rates, the sensitivity to core inventory is strikingly

different for the reasons explained in detail in section 2.4. The neutron flux density in the fuel containing the plutonium is very different for the two configurations of the IRT with and without the breeding targets. Since the change in plutonium fission rates is relatively small between these two configurations, we have to conclude that neutrino safeguards is not effective in determining which configuration is used. Therefore, the spread in plutonium mass predictions between the two configurations has to be taken as error, which is 0.36 kg, over one 250 day run. Taking the upper end of the range of plutonium produced in the IRT⁷⁹ of 4 kg, we see that this requires about 8-10 reactor cycles. Since the errors from a neutrino measurement between each cycle are statistically independent we find the total error from a neutrino measurement taking 8 cycles to be $0.36 \text{ kg} \sqrt{8} = 1.0 \text{ kg}$. In the more realistic case of no plutonium production in the IRT this measurement translates into an upper bound of the same size from this source.

5.3 5 MW_e reactor power measurement at IRT

An additional benefit of having a neutrino detector at the IRT reactor is that it would also be sensitive to neutrinos from the 5 MW_e reactor. This is particularly useful during times when the IRT is shut down, which happens for approximately 100 days every year.⁸⁰ This will yield two measurement periods of 100 days each for the reactor power of the 5 MW_e reactor during the crucial time, after the 70 d shutdown and before the first inspection, where the declared power was low, around 8 MW_{th}, but would have been as high as 18 MW_{th}, in order to bring the second core to the same final burn-up, see figure 5.

Data collection is assumed to start shortly after an IRT shutdown at a point where all but the long-lived neutrino producing isotopes have decayed away, leaving only the LLI: strontium-90, ruthenium-106, and cerium-144. This occurs on the order of days. The number of atoms for each of the LLI was computed using SCALE and is shown in table III. As in

79. Albright and O'Neill, *Nuclear Puzzle*, p. 120.

80. Ibid., pp. 148-149.

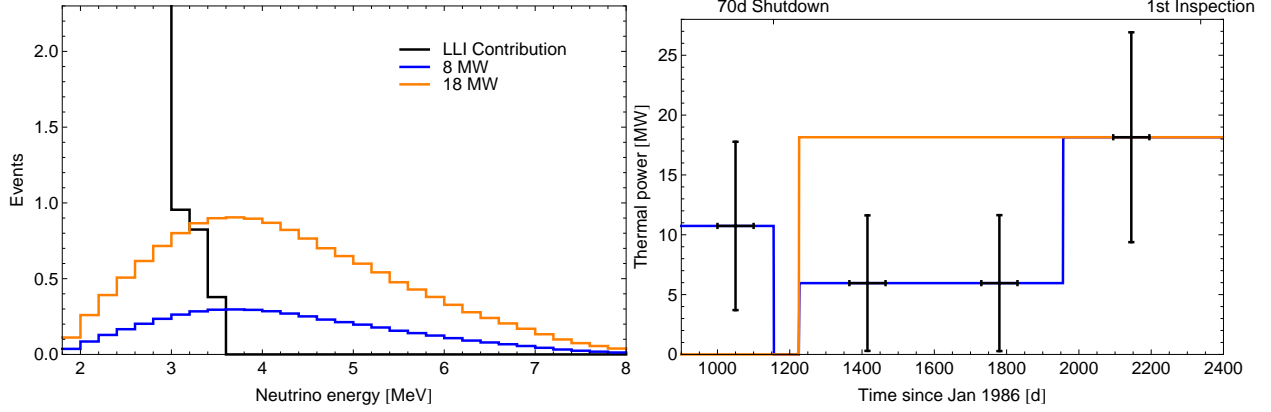


Figure 9: In the left hand panel events are shown for 200 days of data collection 20 m from the shut down IRT reactor and 1.2 km from the running 5 MW_e reactor. The IRT is assumed to only contribute to the detected neutrino spectrum through its long lived isotopes shown in black. The 5 MW_e reactor is assumed to be running either at the declared 8 MW_{th}, as shown in blue, or at 18 MW_{th}, as shown in orange. The right hand panel shows the 1 σ sensitivities to reactor power resulting from this measurement. The blue curve shows the power history under the assumption of no diversion. The orange curve shows the power history if there had been diversion.

Table III: Number of long-lived isotope atoms assumed shortly after IRT shutdown.

Isotope	strontium-90	ruthenium-106	cerium-144
Amount (atoms)	3.4×10^{23}	2.8×10^{22}	2.5×10^{23}

the previous sections, we use a 5 t detector at 20 m standoff from the IRT and 1.2 km from the 5 MW_e reactor, see figure 4. Data is collected over two 100 day periods and the detected spectrum is shown in the left hand panel of figure 9. The signal event numbers are small and therefore we use the appropriate Poisson log-likelihood to define the χ^2 -function

$$\chi^2 = 2 \sum_i [n_i \log \frac{n_i}{n_i^0} - (n_i - n_i^0)] \quad \text{with} \quad n_i = N P_{\text{th}} \sum_I F_I S_{I,i} + LLI_i, \quad (14)$$

where LLI_i is the long lived isotope contribution in the bin i . Resulting sensitivities are shown in the right hand panel of figure 9. This corresponds to an uncertainty of about 3.8 MW_{th} during the periods of interest. The difference in reactor power for a second core would be detected at 3.2 σ .

This result implies that a larger detector could be used to safeguard several reactors

in a larger area. In particular, a detector that is sensitive to direction could identify the reactor that contributed the neutrino and get several power measurements simultaneously. Also, without the need to be close to a reactor, it could be placed underground allowing for greater background reduction.⁸¹

5.4 Waste detection

In addition to directly monitoring reactors, neutrino detectors can be used for detection of nuclear waste. With sufficient insight of where waste might be disposed, a nearby neutrino detector can see the signature of LLI, even after years of storage. Table IV lists the number of atoms of each of the three primary LLI that would be expected in the waste at the point in time of the first inspection, roughly 3 years after the 70 day shutdown. In the following analysis, it is assumed that the complete core was removed during the 70 day shutdown and the resulting reprocessing wastes are stored together in one of three locations: the “suspected waste site”, building 500, or the Radiochemical Laboratory.⁸² All three locations are shown in figure 4. For building 500, we assume that we can not deploy inside the hatched area, since this facility was declared to be a military installation exempt from safeguards access.⁸³ The resulting standoff distances are shown in table V.

Table IV: Number of long-lived isotopes at day 2251 for a complete reactor core removed at day 1156 and stored for 3 years.

Isotope	strontium-90	ruthenium-106	cerium-144
Amount (atoms)	1.2×10^{24}	1.4×10^{22}	3.7×10^{22}

Due to the low event statistics, a Poisson log-likelihood is used, as in equation 14, with the difference that the reactor events from the 5MW_e are now background and the signal are the LLI_i . Table V summarizes the results for each location. Figure 10 shows the event

81. Jocher et al., “Theoretical antineutrino detection, direction and ranging at long distances.”

82. Albright and O’Neill, *Nuclear Puzzle*; O. Heinonen, Interview by PH, April 16 2013, Heinonen does not believe that the liquid, high-level waste was transferred to building 500.

83. Albright and O’Neill, *Nuclear Puzzle*, pp.149-154.

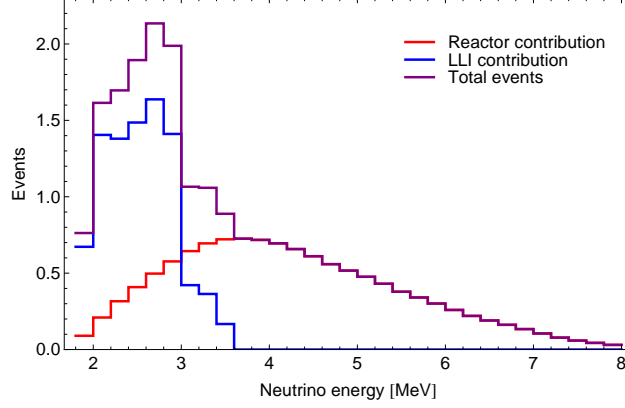


Figure 10: Total event rates are shown in purple for 1 year of integrated data collection starting in 1992 with a 5 t detector 25 m from spent fuel and 1.83 km from the 5 MW_e reactor. The reactor contribution to total event rates are shown in red and long lived isotope contributions shown in blue.

rate spectrum in the most promising of the setups considered, the case of the reprocessing plant. It is found that a detector around 25 m from the waste and 1.8 km from the 5 MW_e reactor would have a 2σ signal after 55 days of data collection. The strongest contributor to detection capability is the distance from the source.

Table V: Events are integrated over 1 year with a 5 t detector. The waste corresponds to a complete reactor core discharged in 1989 during the 70 day shutdown. Long lived isotopes are decayed 3 years before the measurement starts. The expected time to achieve a 2σ detection is given in the last column.

Location	Reactor Distance [m]	Fuel Distance [m]	Reactor Events	Fuel Events	χ^2	2σ Time [y]
Building 500	1980	80	10.1	0.9	0.34	≥ 10
Suspected Waste Site	1060	25	35.3	8.9	8.22	0.33
Reprocessing Plant	1830	25	11.8	8.9	16.95	0.15
Reprocessing Plant	1800	100	12.2	0.6	0.12	≥ 10

5.5 Continuous neutrino observations

In applying neutrino safeguards, like in conventional safeguards, we can use individual measurements taken at different times and apply them in combination to infer what actually happened. The initial declaration to IAEA by the DPRK admits two extreme cases: both a

very minor discharge of a few hundred fuel elements and a complete core discharge in 1989 would yield the same overall core configuration at the time inspectors arrived in 1992, see figure 5.

The real strength of a neutrino detector is evident when it can measure over the history of a reactor. As seen in figure 6, such a detector is capable of being very sensitive to reactor power. Thus, if a neutrino detector was present for the lifetime of the reactor, the declared power would have to match the measured power at all times and, since the burn-up is just the time integrated thermal reactor power, the burn-up could be inferred from a complete power history. At the same time, a burn-up measurement, in contrast to an inferred burn-up value, can also be derived from a neutrino measurement, provided a reliable, but not necessarily very detailed or accurate, reactor model is available. As will be shown in section 6.1, given that the bulk quantities in terms of burn-up are the same between the two scenarios, all conventional methods which can address the issue of the second core also rely on a reactor model. The diversion scenario that has been considered relies heavily upon the ability to adjust the power relative to the declared power so that both the power and burn-up match at a later time. In the presence of a neutrino detector, the difference in burn-up will be frozen between the declared burn-up and the actual burn-up of the new core. The fact that a neutrino detector can simultaneously measure power, as well as fission fractions, is what allows it to detect this difference in burn-up. To determine sensitivity to such a situation, a modified version of equation 13 is used

$$\chi^2 = \sum_t \sum_i \frac{1}{n_{i,t}^0} \left[(1 + \alpha_{\text{detector}}) P_{\text{th}}^t \sum_I F_I(BU^t) S_{I,i} - n_{i,t}^0 \right]^2 + \left(\frac{\alpha_{\text{detector}}}{\sigma_{\text{detector}}} \right)^2. \quad (15)$$

where t is indexing the time interval for which a measurement is available. α_{detector} is a detector normalization parameter with uncertainty σ_{detector} . P_{th}^t is the average reactor power in each time bin t . F_I are the fission fractions which are a function of the burn-up in each

time bin t , BU^t . The burn-up as a function of time is given by

$$BU^t = \left(\sum_{\tau=1}^{t-1} \frac{P_{\text{th}}^{\tau} \Delta\tau}{M_{\text{core}}} \right) + BU^0 \quad (16)$$

where $\Delta\tau$ is the width of the time bin, BU^0 the initial burn-up at the start of data taking and M_{core} the mass of the reactor core in terms of fuel loading. If this initial burn-up BU^0 is well known, as it would be if data collection began at start-up, such an analysis greatly reduces the uncertainty in the total plutonium budget. In table VI, the total error budget is given through the use of this method, labeled “method 2”, and is shown compared to the results if only the burn-up but *not* the power history is measured based on the results of the previous sections, labeled “method 1”. For method 2 we assumed that reactors start with a well known composition, that is $BU^0 = 0$ and a detector related uncertainty $\sigma_{\text{detector}} = 1\%$ is achievable and all the P_{th}^t are free parameters in the fit. In the case of the 5 MW_e reactor, for both analyses, the question is what is the maximum change in BU^x during the 70 day shutdown. The value of BU^x is translated into the resulting plutonium mass sensitivity by using the reactor model. It is clear that method 1 is less accurate but does not rely on continuity of knowledge whereas method 2 is much more accurate but requires continuity of knowledge. Method 2 still offers a significant advantage compared to conventional methods by providing its results in real-time and not only at some later, unspecified time in the future.

For completeness we also list the plutonium mass sensitivities from the indirect method and the detection of reprocessing wastes in table VII.

5.6 Impact of backgrounds

So far in this analysis, we have neglected backgrounds not related to neutrino emissions. The main backgrounds in inverse beta-decay detectors are: accidentals, where two uncorrelated events caused by ambient radiation in the detector accidentally fulfill the delayed coincidence requirements in both time and energy; fast neutron induced backgrounds, where

Table VI: Plutonium content and 1σ uncertainties are given for two analysis techniques for both the IRT and 5 MW_e reactors. Due to the inability to reliably detect the presence of targets in the IRT reactor, they are assumed to be in the reactor. The detection capability is given for each 250 day run of the IRT. The 5 MW_e reactor plutonium error is a combination of removed plutonium that may have occurred during the 70 day shutdown and the final plutonium content in the reactor at the 1994 shutdown. The quantities are independent if data is only taken after the 1st inspection and correlated if taken from start-up. The flat burn-up analysis adds a fixed burn-up to each time bin and the final plutonium error is the final plutonium difference between the burn-up increased data and the expected data. The power constrained analysis assumes the starting fuel composition is known and the burn-up is given by the integration of the power with an assumed 1% detector normalization uncertainty. The plutonium error is the maximum plutonium difference attainable through power increases and fuel removal (in the case of the 5 MW_e reactor). Values are given for 1σ sensitivities for maximizing the plutonium available for core 1 or core 2 respectively. Parenthesis are for uncertainties in cores using only data from the respective section. Core 3 and core 4 are additional fuel loads that are irradiated in the 5 MW_e reactor post-1994 according to Albright and Walrond, *North Korea's Estimated Stocks of Plutonium and Weapon-Grade Uranium* and are added for completeness.

* Using uncertainty from Albright and O'Neill, *Nuclear Puzzle*

† These two numbers are anti-correlated with a correlation coefficient of -0.962.

		Final		Method 1, 1σ		Method 2, 1σ	
Reactor		Burn-up [MWd/t]	Pu [kg]	Burn-up [MWd/t]	Pu [kg]	Burn-up [MWd/t]	Pu [kg]
IRT/run with targets		3550	0.47	3520	0.47	39	0.01
5 MW _e from 1st inspection	Core 1	178	8.83	178	9.5*	N/A	
	Core 2	648	27.7	95	3.29		
5 MW _e from start-up	Core 1	178	8.83	138 (83)	6.68 (3.76 [†])	43 (1.9)	2.12 (0.11)
	Core 2	648	27.7	52 (66)	1.81 (2.30 [†])	6.7 (6.9)	0.23 (0.24)
5 MW _e Core 3		307	14.6	51	2.17	3.2	0.14
5 MW _e Core 4		255	12.3	53	2.36	2.7	0.12

a fast neutron enters the detector without leaving trace and scatters off a proton, which then is confused with the primary energy deposition of a positron, and subsequently the neutron thermalizes and captures like a genuine neutron from inverse beta-decay; β -n backgrounds, where interaction with cosmic ray muons produces a short-lived radioactive isotope which decays by beta-delayed neutron emission, which mimics a neutrino event. The rate of accidentals is determined by the rate of ambient radioactive decays. Fast neutrons are a result of cosmic ray interactions in materials surrounding the detector and thus depend on the rate of cosmic ray muons; the same is true for β -n backgrounds. Therefore, the measured

Table VII: 1σ uncertainties on the discharged plutonium for core 1 for the IRT parasitic measurement and for the detection of high-level reprocessing waste.

		Core 1 burn-up [MWd/t]	Core 1 Pu [kg]
Waste measurement	Parasitic measurement	51	2.55
	Suspected waste site	56	2.76
	Reprocessing plant	34	1.67

background rates due to those two sources have to be scaled from the underground location, where most current neutrino detectors are located, to the surface. Neutrino detectors are commonly put underground precisely to reduce these two sources of backgrounds, since deep underground the cosmic muon flux is strongly attenuated. The scaling of the number of background events is not purely given by the muon flux, but also, to some degree, depends on the average muon energy,⁸⁴ the scaling is given by

$$R \propto \phi_\mu \langle E_\mu \rangle^\alpha, \quad (17)$$

where ϕ_μ is the muon flux and $\langle E_\mu \rangle$ is the average muon energy which, at the surface, are $127 \text{ m}^{-2} \text{ s}^{-1}$ and 4 GeV , respectively.⁸⁵ α ranges from $0.7 - 0.9$ depending on the type of background. Using the numbers measured in the Double Chooz experiment at a depth corresponding to 300 meter water equivalent (mwe)⁸⁶, we can scale to a surface deployed detector and find $1 \text{ d}^{-1} \text{ t}^{-1}$ fast neutron events and $43 \text{ d}^{-1} \text{ t}^{-1}$ β -n events, where 1 tonne is assumed to have the composition of CH_2 . These rates exceed the accidental rates by a large factor and therefore we can neglect the accidental backgrounds. This scaling is tested against several data sets from different experiments spanning a depth range from $850 - 120 \text{ mwe}$ and the scaling is found to be accurate within a factor of two.⁸⁷ At very shallow depths of less

84. Y. Abe et al., “Direct Measurement of Backgrounds using Reactor-Off Data in Double Chooz,” *Phys.Rev. D*87 (2013): 011102, doi:10.1103/PhysRevD.87.011102.

85. J. Beringer et al., “Review of Particle Physics (RPP),” *Phys.Rev. D*86 (2012): 010001, doi:10.1103/PhysRevD.86.010001.

86. Overburden is commonly quoted in units of meter water equivalent (mwe), typically 1 m of rock/soil corresponds to about 2-3 mwe.

87. Abe et al., “Backgrounds.”

than 10 mwe, the hadronic component of cosmic radiation is non-negligible and the scaling relation in equation 17 is probably no longer valid. With this caveat in mind, we show in table VIII the noise to signal ratios for the various detector deployment scenarios. Values smaller than 1 indicate that the current detector technology is likely to be sufficient and values larger than 1 indicate that improvements in background rejection are needed. The

Table VIII: Noise to signal ratios for a surface deployed detector.

Source	Fast neutron suppression	β -n suppression
5MW _e	0.07	0.21
IRT	0.14	0.43
IRT parasitic	260	1050
Waste	740	3080

required rejection factor can be reduced significantly by providing a moderate overburden of 10-20 mwe, which, in principle, can be engineered into the detector support structure.

Fortunately, there is a significant on-going experimental effort in several countries to address the R&D for neutrino detectors with greatly improved background rejection. These initiatives are motivated by the search for a new particle called a sterile neutrino⁸⁸ through the use of neutrinos from reactors with detectors placed within meters of the reactor core. The close proximity to a reactor core results in a high-background environment which can include a significant flux of fast neutrons and high-energy gamma-rays from the reactor itself. Almost all reactor sites under consideration offer only very minimal overburden of 10 mwe or less. Therefore, these experiments face essentially the same level of problems in terms of signal to noise conditions as safeguards detectors would under the conditions outlined in this paper. Specifically, there are, to name but a few, the PROSPECT collaboration in the U.S.,⁸⁹ the DANSS⁹⁰ project and NEUTRINO-4⁹¹ in Russia, the STEREO project in

88. Abazajian et al., “Light Sterile Neutrinos: A White Paper.”

89. Z. Djurcic et al., “PROSPECT - A Precision Reactor Neutrino and Oscillation Spectrum Experiment at Very Short Baselines” (2013).

90. I. Alekseev et al., “DANSSino: a pilot version of the DANSS neutrino detector” (2013).

91. A.P. Serebrov et al., “On possibility of realization NEUTRINO-4 experiment on search for oscillations of the reactor antineutrino into a sterile state” (2013).

France, and the SOLID project in Belgium. Each experiment has chosen a unique approach to address the challenges of a high noise to signal ratio and some experiments have already reached the prototype stage.

6 Application to the 1994 crisis

6.1 Conventional methods

The events in 1994 put a premium on understanding the actual history of the North Korean plutonium program; a vivid interest in this problem remains in the aftermath. The actual text of the Agreed Framework states

[...] before delivery of key nuclear components, the DPRK will come into full compliance with its safeguard agreement with IAEA (INFCIRC/403), [...] with regard to verifying accuracy and completeness of the DPRK's initial report on all nuclear material [...]

Section IV, Paragraph 3

In 1994, and even today, there has been a need to resolve the question of whether there was significant reprocessing prior to 1992. It comes as no surprise that actual methods, relying on more conventional means, were devised. We will briefly review those conventional methods.

The unloading of the 5 MW_e core in June 1994 provided a crucial opportunity to acquire data that would allow a determination of whether there was a partial or complete core unloading in 1989. The DPRK, aware of this possibility, tried to prevent IAEA from gaining this information by unloading the core very quickly and, by doing so, made it impossible to infer the exact position of a fuel element inside the core. Unfortunately, there is little published on the details of how a measurement would have proceeded and we have to rely on interviews with experts. The basic concept of the method is to map out the three dimensional burn-up distribution inside the reactor core. If the declaration by the DPRK, that only a

few hundred damaged fuel elements were replaced in 1989 were true, then there should be a discontinuity in the burn-up distribution at the position of the replaced fuel elements.⁹² On the other hand, if more than those few hundred were replaced then discontinuities would show up at many more locations. If the whole core was replaced a continuous distribution would emerge. Overall, there are about 8,000 fuel elements and the goal is to find a discrepancy concerning as few as several hundred fuel elements. Therefore, a sizable sample of about 300 fuel elements is required.⁹³ There are two principal methods to determine the burn-up of spent fuel: one is destructive sampling with subsequent isotopic analysis and the other is to measure the characteristic radioactivity emanating from a spent fuel element. Destructive sampling was (and is) exceedingly difficult in this context.⁹⁴ The other possibility to measure burn-up relies on measuring gamma-emission from mostly cesium-137, which is a good proxy for burn-up. According to an expert from Los Alamos National Laboratory who was closely involved in the 1994 DPRK issue, this technique would provide burn-up errors below 5% if good quality calibration data existed.⁹⁵ This method, in principle, has been calibrated on British Magnox fuels. Applying this type of measurement to several hundred of the spent fuel elements and knowing their location in the core presents a viable method to reconstruct the three dimensional burn-up distribution. None of the interviewed experts was willing to make a statement as to what level of precision, in terms of partial core reloads and extracted plutonium amounts, would have resulted. However, we can put a lower limit on the achievable error by assuming that the overall systematic errors are less than 5% and the errors for individual fuel elements are in the 1-5% range.⁹⁶ Therefore, the overall accuracy very roughly should be in 1-5% range.

This estimate coincides with the accuracy of a method which is based not on the sampling of spent fuel but instead on sampling the graphite moderator in the reactor. The idea is

92. Heinonen, *Interview*; B. Reid and C. Gesh, Phone interview by PH, May 15 2013.

93. Wit, Poneman, and Gallucci, *Going Critical*, p. 170.

94. Reid and Gesh, *Interview*.

95. H. Menlove, private communication.

96. Ibid.

elegant and simple; the graphite moderator is in the reactor for the entire lifetime of the reactor and thus it will be exposed to *all* the neutrons produced throughout the history of reactor operation. Since plutonium results from neutron capture on uranium-238, the total amount of plutonium produced is strictly proportional to the number of all neutrons. Even reactor grade graphite contains traces of other elements like boron or titanium and both these elements have stable isotopes, specifically boron-11 and titanium-49, which result from neutron capture. Therefore, the ratios boron-10/boron-11 and titanium-48/titanium-49 will decrease with the total neutron fluence. This graphite isotope ratio method (GIRM) was first proposed by Fetter in 1993⁹⁷ and subsequently developed in considerable detail at Pacific Northwest National Laboratory. In an actual application, samples from the graphite would be taken at a few hundred strategically chosen points throughout the core and the isotope ratios would be determined by mass spectroscopy. This data then can be used to reconstruct a three dimensional neutron fluence distribution which then, in turn, can be converted to the total amount of plutonium produced in the reactor through its entire lifetime. This method was experimentally verified at a British reactor⁹⁸ with an accuracy in the 1-5% range.⁹⁹ This method is quite invasive and requires extensive cooperation between the national authorities and operator of a reactor in question, and the state or organization carrying out the testing. It has the advantage that it is tamper resistant and the historical record, in the form of the graphite moderator of the 5 MW_e reactor, is still available.

We have reviewed two methods: one based on gamma-ray emission of spent fuel and the other on isotope ratios in the graphite moderator. Both methods rely on several hundred samples collected across the reactor and a subsequent reconstruction of three dimensional distributions of either burn-up or neutron fluence. For the first method we can only provide a rough estimate of accuracy, whereas for GIRM the errors have been experimentally deter-

97. Steve Fetter, “Nuclear Archeology: Verifying Declarations of fissile-material production,” *Science and Global Security* 3 (1993): 237–259.

98. Bruce Reid et al., *Trawsfynydd plutonium estimate*, 13528, technical report (Pacific Northwest National Laboratory, 1997).

99. Patrick Heasler et al., “Estimation procedures and error analysis for inferring the total plutonium (Pu) produced by a graphite-moderated reactor,” *Reliability Engineering and System Safety* 91 (2006): 1406–1413.

mined; the rough estimate and the experimentally determined error are in the same range of 1-5%. The method relying on spent fuel measurements ultimately requires additional information, e.g. that a few hundred rods were exchanged in 1989, to make inferences about alternative core histories which lead to the same total burn-up. The GIRM method, on the other hand, can directly address the cumulative plutonium production in the core and thus does not rely on additional information. Comparing this to the results that can be obtained from neutrino measurements, see table VI, we see that neutrino measurements, which do not rely on knowing the core history, reach about 15% accuracy based on the burn-up of a given core. Again, for alternative fuel histories which lead to the same burn-up, this method requires additional information. If the whole fuel cycle can be monitored the neutrino accuracy improves to about 1%. The overall accuracy of neutrino measurements falls in the same general range as those achievable by conventional means. Each of the techniques considered here has different requirements for additional information to resolve equal-burn-up alternative fuel histories, only GIRM can resolve those without extra information.

Another marked difference is the level of intrusiveness, which in descending order goes from GIRM, which requires drilling sizable holes into the moderator; to the sampling of spent fuel, which requires considerable access during refueling; and then to neutrino monitoring, which only requires access to the exterior of the reactor building. Also, neutrinos are the only method providing essentially real-time information, a significant advantage in the context of break-out scenarios. Up to the point of the break-out, all information is available, whereas for the conventional methods, the information can be obtained only at very specific points in time, well after the actual plutonium production took place. If the break-out happens between the time of plutonium production and the time when conventional means can be applied, no information is obtained at all – like in the case of the DPRK.

6.2 Neutrinos

Based on the quantitative results and the time-line of events in 1994, see figure 3, the following scenario may have been put into effect:

- The IRT is under full neutrino safeguards with a dedicated 5 tonne detector from 1978 on, which is located outside the IRT reactor building at the southern wall.
- The 5 MW_e is under full neutrino safeguards with a dedicated 5 tonne detector from May 1992 on, which is located outside the 5 MW_e reactor building at the western wall.
- A search for neutrino emissions from the reprocessing waste is initiated in November 1992. Three 5 tonne detectors are deployed: one at the reprocessing plant; one at the suspected waste site, located above the center of the waste site; and one at building 500, located right outside the southern fence.

This scenario is fully consistent with the *actual* safeguards access the IAEA had and, in particular, all detector deployment locations reflect actual physical access. As a result, the detectors at the IRT and 5 MW_e have a standoff of 20 m, the detectors at the suspected waste site and reprocessing plant have a distance of 25 m, and the one at the building 500 has a distance of 80 m.

Furthermore, we assume that in 1989 the DPRK discharged the complete first core, which seems to be corroborated by the declaration of the DPRK in 2008 that it possesses 30 kg of plutonium.¹⁰⁰ After reprocessing of the spent fuel, the waste was stored somewhere in the reprocessing plant.¹⁰¹ Finally, we also assume that the burn-up declared by the DPRK in 1992 is indeed correct.¹⁰² This completely specifies the scenario.

The first relevant piece of data would be obtained by the IRT detector during periods when the IRT is shut down, about 100 days out of each year. The neutrino signal stemming

100. Albright and Walrond, *North Korea's Estimated Stocks of Plutonium and Weapon-Grade Uranium*.

101. Heinonen, *Interview*.

102. Albright and O'Neill, *Nuclear Puzzle*; Heinonen, *Interview*.

from the operation of the 5 MW_e is clearly detectable at this detector location and provides a measurement of reactor power. In 1989, this signal would have been recorded but would not have raised any special concern, since the 5 MW_e was not under safeguards at this time. At most, this data would have helped to corroborate U.S. government analyses of satellite imagery to ascertain the operational history of the 5 MW_e. However, soon after the DPRK had submitted its initial declaration to the IAEA, in May 1992, this data would have resulted in a discrepancy which, in combination with the results from environmental sampling would have led to the conclusion that a large amount of plutonium had been separated in 1989. This measurement, according to table VII, has a sensitivity which corresponds to 2.55 kg plutonium, or equivalently to a $8.83/2.55 = 3.5\sigma$ detection, meaning the IAEA would have known that a significant fraction of the first core had been discharged with a confidence of 1 in 1 900. Taking 4 kg of plutonium as the quantity needed for a nuclear bomb, this result translates into a 1 in 13 confidence that the DPRK has at least enough plutonium for one bomb.

In November of 1993, after a year of data collection, the detectors at the suspected waste site would not have found anything nor would the detector at building 500, the former result proving that only a small amount of high-level waste could be present at the suspected waste site and the latter being insignificant since the distance to the waste is too large. The detector at the reprocessing plant would have shown the presence of high-level radioactive waste,¹⁰³ corresponding to a plutonium accuracy of 1.67 kg. That is, with a confidence of 1 in 1,000,000, the presence of reprocessing waste would have been confirmed. Moreover, with a confidence now of 1 in 270, it would have been known that enough plutonium for one weapon was processed. Six months later, in May 1994, the 5 MW_e detector would have confirmed the burn-up declaration of the DPRK with an accuracy of 15%. In combination, these results would have implied a 56% chance of there being enough plutonium for two or

103. Heinonen, *Interview*; Siegfried Hecker, *Report of Visit to the Democratic People's Republic of North Korea (DPRK) Pyongyang and the Nuclear Center at Yongbyon, Feb. 12-16, 2008.*, technical report (Center for International Security and Cooperation, 2008).

more bombs.

Overall, had the DPRK allowed the detectors to be installed and operated, neutrino safeguards would, in the scenario considered, have changed the state of information significantly. The existence of a separate first core would have been established with very high confidence and the fact that this core was reprocessed would have been known to very high confidence. It would have been known, with very high confidence, that at least enough plutonium for one bomb has been separated. There would have been some indication that there would be enough separated plutonium for two bombs. Again, if the DPRK had allowed the use of neutrino detectors, all of this knowledge would have been available by the end of 1993.

Assessing the impact this additional knowledge would have had on the course of events and the policies driving those events is difficult and will have to remain speculative. From an IAEA perspective, the DPRK would have been found in substantial violation of the NPT and the Director General would have to report his findings to the Board of Governors and, as result, the matter would have been referred to the UN Security Council. Furthermore, the history of the North Korean plutonium production would have been known including a reasonably accurate account of the amount of separated plutonium. The ability of the IAEA to deliver such a detailed picture, despite extensive efforts on the side of the DPRK to obfuscate, in a timely manner would have been counted as a major success.

As far as the U.S. and the DPRK are considered, we note that the primary goals and motivations would have remained invariant for both sides. The U.S. still would have wanted to prevent any further production of separated plutonium¹⁰⁴ and the DPRK still would have wanted to obtain maximal material and political gains for eventually accepting any U.S. demands. Both parties would have remained keen to avoid war on the Korean peninsula, since for the U.S. the number of casualties and financial burden would have appeared difficult to justify and a war would clearly be against the interest of its close ally South Korea. For the DPRK, or more specifically its leadership, a war would constitute the ultimate catastrophe

104. R. Gallucci, Interview by PH, April 17 2013, According to Gallucci the main objective of the U.S. at all stages of the 1994 crisis and the subsequent negotiations was to prevent any further plutonium production.

resulting in regime change, at a minimum, and likely captivity or worse for the very top echelons of government. These stakes remain for both sides to this day and the mutual awareness thereof has provided some measure of stability to the Korean peninsula.

In view of the information provided by neutrinos, both parties would have lost the benefit of ambiguity, which would have forced the U.S. to act decisively. For North Korea, it would have become much more difficult to pretend that a mere accounting problem had occurred. As a result, the tension would likely have risen much more sharply resulting in the peak of the crisis at a much earlier time, now the fall of 1993 instead of June 1994.

There are many arguments which can be levied against the scenario described in the preceding paragraphs. On the technical side, neutrino detectors which achieve the required level of background rejection did not exist in the 90s and do not exist now, at least not with demonstrated capabilities. In reply to this criticism we point to the discussion in section 5.6, where also a brief summary of the current R&D efforts toward better detectors is given. On the historical side, any attempt at counter-factual history ultimately remains a piece of fiction and, while some story lines may be more plausible than others, there is no way to really know what was known by whom given the actual circumstances, or what differences antineutrino monitoring, as described in this paper, would have made in the interactions and outcomes. On the policy side, safeguards generally do not rely on secret technologies and black boxes. States entering a safeguards agreement with the IAEA have the right to require a complete specification and understanding of the employed technologies to ascertain their right of protection of trade secrets and information that is sensitive with respect to national security. The DPRK is no exception to this rule¹⁰⁵ and its scientists are knowledgeable and competent experts, which certainly would have the ability to understand all implications of neutrino safeguards as outlined here.¹⁰⁶ Given that they made every effort to conceal the true history, they also would have tried to thwart neutrino safeguards. Neutrino safeguards is not necessarily more difficult to thwart than other means, it just requires different counter

105. Reid and Gesh, *Interview*.

106. Heinonen, *Interview*; Reid and Gesh, *Interview*.

measures. This back-reaction has been completely neglected, in part because it would add another layer of speculation and because it is a historical fact that the IAEA's trace analytic capabilities caught the North Korean experts off guard.

7 Summary & Outlook

Neutrino reactor monitoring offers unique capabilities which seem to make this method – as proposed more than 30 years ago – a useful tool for safeguards. Also, neutrino detectors have been continually refined since the days of Cowan and Reines and can be considered a mature technology. Given the mechanisms of neutrino production and detection, neutrino safeguards provide bulk measurements of reactor core parameters like power or burn-up. This is to be contrasted with the current safeguards approach which largely relies on item accountancy and, in particular, neither power nor fuel burn-up are actually measured by the IAEA¹⁰⁷ or verified through independent calculations for any reactor. The IAEA is apparently satisfied that the existing arrangements are adequate for commercial power reactors of the boiling and pressurized water types, especially as long as a once-through fuel cycle without reprocessing is considered. As a result, it has been difficult to show neutrino safeguards would provide a decisive advantage in comparison to more conventional techniques, especially since neutrino detectors are larger and more expensive than most equipment currently used by the IAEA. The fact that, in the literature, a rather diverse set of results, in terms of the applicability to specific safeguards issues, is found¹⁰⁸ may have a further detrimental effect on the perception of neutrino safeguards. These widely varying results can be attributed,

107. Doyle, “Nuclear Safeguards, Security and Nonproliferation: Achieving Security with Technology and Policy.”

108. Bernstein et al., “Nuclear reactor safeguards and monitoring with anti-neutrino detectors”; Nieto et al., “Detection of anti-neutrinos for nonproliferation”; Huber and Schwetz, “Precision spectroscopy with reactor anti-neutrinos”; Misner, “Simulated Antineutrino Signatures of Nuclear Reactors for Nonproliferation Applications”; Bernstein et al., “Nuclear Security Applications of Antineutrino Detectors: Current Capabilities and Future Prospects”; Bulaevskaya and Bernstein, “Detection of Anomalous Reactor Activity Using Antineutrino Count Rate Evolution Over the Course of a Reactor Cycle”; Hayes et al., “Theory of Antineutrino Monitoring of Burning MOX Plutonium Fuels”; Huber, “Spectral antineutrino signatures and plutonium content of reactors.”

to a large degree, on differing assumptions about detector parameters and different level of statistical treatment. The choice of detector parameters often is inspired by the wish to be particularly realistic or thrifty, which seems to be a classical case of what Donald Knuth calls premature optimization.¹⁰⁹ Furthermore, many analyses are rate-based which leads to serious deficiencies in sensitivities since there is a pronounced degeneracy between reactor power and fission fractions when spectral information is ignored¹¹⁰.

In this paper we have taken a different approach – with the North Korean nuclear crisis of 1994 we have identified a real-world scenario in which traditional safeguard techniques ultimately were unable to resolve the key questions and for which sufficient technical information is publicly available to perform a detailed analysis. Moreover, we base our detector parameters on the overall acceptable size and weight of the entire detector system, which we envisage to fit inside a standard 20 ft intermodal shipping container. We also assume that the detector will be able to operate at the surface. Together with the standard packaging this will provide a great deal of flexibility in the choice of deployment locations. The price to pay is that the detector has to have excellent background rejection, which seems to exclude single volume liquid scintillator detectors and favors finely segmented solid detectors, see section 5.6. Detectors with these capabilities currently do not exist, but a basic science question related to the possible existence of a new particle, a so-called sterile neutrino, has triggered a large number of experimental efforts to perform reactor neutrino experiments at a range of several meters from compact reactor cores. These experiments face enormous challenges from reactor-generated backgrounds and, therefore, have to solve the background rejection issue. Many of the new designs do not rely on large-area photo-detectors, which are typically hand-made in small numbers and therefore are very expensive. New detector designs have the potential to become more affordable in industrial production. Therefore, there is ample reason to assume that within a few years detectors with the required characteristics will be

109. Donald E. Knuth, “Computer programming as an art,” *Communications of the ACM* 17, no. 12 (1974): 667–673.

110. cf. compare the results in () with the ones in ()

available at more reasonable prices.

Spectral analysis of neutrino emissions from a reactor requires an accurate understanding of the neutrino yields from fissile isotopes. Recently, there have been a number of publications addressing the issue of neutrino yields and many of the previously accepted results from the late 1980s have been called into question. In section 2.2, we point out, that while the absolute neutrino yields differ significantly between different calculations, the differences in neutrino yields between the fissile isotopes are predicted quite consistently. Ultimately, these questions should be settled by a calibration measurement at a reactor with well-known core composition.

In section 2.4, we developed a quantitative framework to determine the plutonium mass inventory of a number of different reactor types from neutrino spectroscopy and based our study on detailed reactor burn-up simulations. In figure 2, we summarized these results as a function of the reactor thermal power for an analysis which makes no assumptions about the history of reactor power. In comparing various reactor types and their suitability for neutrino safeguards, we identified the neutron flux density, which is closely related to the power density, as the main parameter of influence.

We showed that antineutrino safeguards could enable the IAEA to detect unreported plutonium production or diversion of declared plutonium at the one significant quantity amount, i.e. 8 kg of plutonium within 90 days at 90% confidence level at light-water moderated reactors producing less than 1 GW_{th} power and at heavy-water moderated reactors producing less than 0.1 GW_{th} power. These results suggest that the heavy-water reactor at Arak in Iran with an estimated thermal power of 0.04 GW_{th} could be an ideal target for neutrino safeguards, and a detection limit of 4.4 kg plutonium within 90 days at 90% confidence level seems possible. Graphite moderated reactors, on the other hand, are more difficult due to a relatively low power density.

We also developed an analysis method based on the fact that the isotopic abundance of the various fissile isotopes as a function of burn-up is governed by reactor physics and conse-

quently these quantities are correlated in a well-defined manner, as explained in section 2.3. In this case, the problem can be rephrased in terms of reactor power and burn-up and this improves the sensitivity by roughly a factor of two. The reactor model required for this type of analysis does not have to be extremely detailed or accurate, since only the gross burn-up evolution is required.

For our purposes, the North Korean nuclear program consists of three pieces: the IRT, an 8 MW_{th} light-water research reactor supplied by the USSR, which is fueled with HEU and has been under IAEA safeguards since 1977; the 5 MW_e reactor, a 20 MW_{th} graphite moderated natural uranium fueled reactor; and the Radiochemical Laboratory, a reprocessing facility which can extract plutonium from the spent fuel using the PUREX process. The central question was whether the fuel in the 5 MW_e reactor was the original core load or whether there was an earlier undeclared refueling during the shutdown in 1989. The discharged fuel would have yielded about 8.8 kg of plutonium, sufficient for at least one nuclear bomb. Our technical analysis is to a large degree based on the data presented in *Nuclear Puzzle*, which we use as input for detailed reactor core simulations for both the IRT and the 5 MW_e reactors.

The North Korean declaration of the burn-up history of the 5 MW_e is such that the core configuration in terms of measurable quantities like burn-up and reactor power is virtually identical for both the one-core and two-core scenarios. Therefore, safeguards techniques, both conventional and neutrino-based, have to resort to secondary observables. In the case of neutrinos, secondary signatures focus on a measurement of reactor power by a neutrino detector deployed to implement the safeguards agreement for the IRT, which has been in force since 1977. This signal is visible only when the much closer and, hence, brighter neutrino source represented by the IRT is not in operation, which occurs for about 100 days per year. This measurement would provide evidence for the presence of a second core with a confidence of 1 in 1 900 (3.5σ), see section 5.

Another secondary signature, which can be exploited with neutrinos is the detection of the presence of reprocessing wastes, which contain long-lived fission fragments, some of

which emit detectable neutrinos. Historically, three sites have been suspected to be the potential disposal locations: Building 500, a suspected waste site, and the Radiochemical Laboratory. The map in figure 4 shows the relative locations. For the latter two sites a neutrino safeguards detector would have been able to detect the presence of the reprocessing wastes with a confidence of better than 1 in 600, see section 5. For the 1994 crisis, the application of neutrino safeguards could have resulted in significantly reduced uncertainty about North Korean intentions.

In a more general context, we also studied the resulting sensitivities assuming that neutrino safeguards had been available from the start-up of the 5 MW_e reactor and showed that if a continuous measurement of reactor power by neutrinos had been available, which could then be compared to a measurement of the burn-up by neutrinos at a later point, there would have been very little room for undeclared plutonium production or refuelings; accuracies corresponding to 1-2 kg of plutonium would have been achieved, see table VI. Our work shows that even graphite moderated reactors can be safeguarded successfully using neutrino monitoring. Furthermore, we compared the abilities of neutrino safeguards with conventional capabilities in section 6.1 and found that those conventional techniques have to rely on a level of reactor physics modeling comparable to the more advanced analysis techniques we have presented. Provided the extensive effort and funds required for such modeling can be expended, the overall accuracy of conventional techniques should be in the 1-5% range, whereas neutrino techniques are in the 5-15% range in terms of plutonium content. The crucial advantage neutrino safeguards offer stems from the near real-time data acquisition during reactor operation, whereas the conventional methods require a reactor shutdown and a defueling of the reactor. Neutrino safeguards also is entirely non-invasive; at 20 m standoff the detector can be deployed outside the reactor building. In the context of break-out scenarios, deferring the ability to know how much plutonium was produced or whether a diversion has taken place until a later point in time, when there is no guarantee of safeguards access at the required level, is problematic – but this is what conventional techniques have

to rely on and have done in the case of the DPRK, with the known result.

To summarize, using the North Korean nuclear crisis as a virtual laboratory, we have found by detailed technical analysis that neutrino safeguards for water moderated reactors with a thermal power less than $0.1\text{--}1\text{ GW}_{\text{th}}$ can meet the IAEA detection goals in terms of plutonium content and timeliness. This makes neutrinos a viable choice for many research reactors, small, e.g. 40 MW_{th} , plutonium production reactors, and for most of the planned commercial small modular reactors. Small modular reactors would allow for the inclusion of a neutrino safeguards system at the design stage. In the specific North Korean case, we find that neutrinos provide an accuracy which is marginally worse than conventional methods and, qualitatively, the difference in accuracy seems to be irrelevant. At the same time, neutrinos allow conclusions about the plutonium content and potential diversion to be drawn in close to real-time, whereas conventional methods provide the information only after the fact, once the reactor is shut down and defueled. For all of these applications, neutrino detectors have to work with minimal or no overburden and the lower the residual background is, the more versatile the resulting system will be. For very low background detectors, remote power measurements and the detection of reprocessing wastes becomes an attractive possibility, in particular for purposes of nuclear archaeology.

Acknowledgements

We thank R. Gallucci, C. Gesh, O. Heinonen, H. Menlove and B. Reid for their willingness to be interviewed for this project. We also thank A. Erickson, L. Kalousis, J. Link, C. Mariani and in particular T. Shea for their expert opinions on many of the technical issues involved regarding nuclear reactors, neutrino detectors, and safeguards. We thank M. Fallot for providing reactor neutrino fluxes in machine readable format and we also acknowledge useful discussions about solid, segmented neutrino detectors with A. Vacharet and A. Weber. This work was supported by the U.S. Department of Energy under contract DE-SC0003915 and

by a Global Issues Initiative grant by the Institute for Society, Culture, and Environment at Virginia Tech.

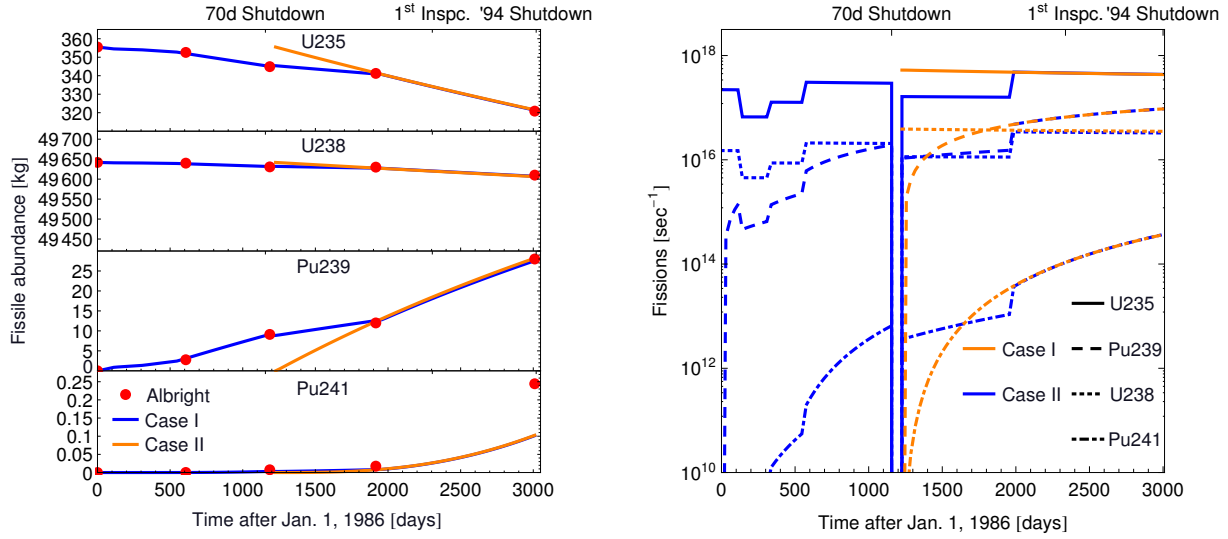


Figure 11: Fissile content of the 5 MW_e reactor (left hand panel) and the corresponding fission rates (right hand panel)

A The 5 MW_e reactor

The 5 MW_e reactor is a graphite moderated and reflected Magnox reactor using natural uranium fuel, based on the British Calder Hall design, and runs with a nominal power capacity of 20-25 MW_{th}. The average burn-up of the fuel elements is 635 MWd/t. The 5 MW_e reactor contains 812 vertical channels, each with up to 10 fuel elements per channel. The fuel elements are made of natural uranium in a magnesium-aluminum alloy (Magnox) and a full core consists of 50 MTU. We have based most of our historical information regarding this reactor and its power history on figure VI.2 in *Nuclear Puzzle*. The 5 MW_e reactor began operation in January 1986, experienced a 70 day shutdown in 1989, and continued irradiation past the first IAEA inspections in 1992 until the shutdown in April 1994. We are primarily concerned with two possible fueling histories: case I, or the no-diversion case, assumes that the same core was used in the 5 MW_e reactor during the entire irradiation period from 1986 to 1994; case II, the core exchange case, is based on the assumption that, during the 70 day shutdown of 1989, North Korea replaced the irradiated core with a fresh one and continued

irradiation with a higher-than-declared power to reach the same burn-up as in case I by the time of the 1992 inspection. The primary safeguards-relevant difference between these two cases is that in the second case an entire spent fuel load containing about 8.8 kg of weapons-grade plutonium, is unaccounted for.

We simulate the 5 MW_e reactor using the SCALE 6.1.1 software package¹¹¹ developed at Oak Ridge National Laboratory. OrigenArp, a subset of SCALE, uses decay data from ENDF/B-VII¹¹² and neutron information from the JEFF/A-3.0¹¹³ databases to compute burn-up and isotopic composition. OrigenArp is a deterministic approach which approximates the structure of a reactor core into a zero-dimensional object by using appropriately weighted cross section libraries. Some libraries, including the Magnox type reactor, are predesigned and supplied with the SCALE software.

OrigenArp begins by computing depletion equations for each individual isotope in a given problem. The depletion or Bateman equation is given by

$$\frac{dN_i}{dt} = \sum_{j=1}^m l_{ij} \lambda_j N_j + \bar{\Phi} \sum_{k=1}^m f_{ik} \sigma_k N_k - (\lambda_i + \bar{\Phi} \sigma_i) N_i \quad (i = 1, \dots, m) \quad (18)$$

This accounts for processes that produce nuclide N_i in the first two terms and for processes that destroy nuclide N_i in the last, negative term. The first term represents the decays of nuclide j to i given by the decay constant, λ_j , the atom density of nuclide j , N_j and the branching fraction, l_{ij} , for decays from nuclide j to i . The second term indicates neutron captures into nuclide i given by the space and energy-averaged neutron flux, $\bar{\Phi}$, the fraction of absorption on nuclide k that produce nuclide i , f_{ik} , and the spectrum-averaged neutron absorption cross section of nuclide k , σ_k . The last term is the collection of depletion modes consisting of the decay of nuclide i via decay constant, λ_i , and neutron absorption with a spectrum-averaged neutron absorption cross section of nuclide i , σ_i . The indices are summed

111. "SCALE."

112. "ENDF database," <http://www.nndc.bnl.gov/exfor/endl00.jsp>.

113. "JEFF database."

Table IX: Comparison of our SCALE-based results and the numbers presented in *Plutonium 1996* for the plutonium content of Magnox fuel as a function of burn-up.

Burn-up [MWd/t]	SCALE % ^{240,241,242} Pu	<i>Plutonium 1996</i> % ^{240,241,242} Pu	SCALE kg of Pu	<i>Plutonium 1996</i> kg of Pu
100	0.99	0.75	0.10	0.1
200	1.9	1.5	0.20	0.19
300	2.9	2.3	0.29	0.28
400	3.8	3.1	0.38	0.36
500	4.7	3.7	0.47	0.45
600	5.5	4.4	0.56	0.535
700	6.4	5.1	0.64	0.62
800	7.2	5.7	0.72	0.7
900	8.0	6.3	0.79	0.78
1000	8.8	6.9	0.87	0.86
1100	9.5	~7.5	0.94	~0.94
1200	10	~8.1	1.0	~1.02

over all branches including nuclide i . SCALE solves this differential equation via a matrix exponential method. Short-lived isotopes are removed to prevent loss of numerical accuracy and calculated using Bateman chains. With the input of initial nuclide concentrations, the power history, and the reactor configuration, OrigenArp can provide time-dependent fission rates, radioactivity, and isotopic abundances during and after irradiation.

For our calculations, we have used the Magnox library provided with SCALE. Our first check of SCALE is to investigate the production of plutonium in comparison to earlier results.¹¹⁴ We irradiate the Magnox fuel corresponding to 1 MTU of natural uranium for 1000 days at a constant power level to reach a given final burn-up. For example, we can irradiate the core at 0.7 MW for 1000 days to produce a final burn-up of 700 MWd/t. We then extract the total amount of plutonium produced and the percentage of ²⁴⁰Pu, plutonium-241, and ²⁴²Pu. table IX summarizes the results and compares them with table A.2 in *Plutonium 1996*¹¹⁵. We can see that our calculation and the results of *Plutonium 1996* consistently match in the total mass of plutonium produced for various burn-ups. SCALE predicts about

114. David Albright, Frans Berkhout, and William Walker, *Plutonium and highly enriched uranium 1996: world inventories, capabilities and policies* (Oxford University Press, 1997).

115. The numbers in *Plutonium 1996* are originally taken from ()

25% more of the lesser plutonium isotopes compared to *Plutonium 1996*.

We also perform a comparison of the fissile abundances for the four main fissile isotopes with the numbers quoted in table VIII.5 in *Nuclear Puzzle*. We use the OrigenArp sequence with the Magnox reactor library and the power history inferred from figure VI.2 of *Nuclear Puzzle* with an initial fuel amount of 1 MTU. The x-axis of the plot shows the number of days that have passed after the 5 MW_e reactor began irradiation on January 1, 1986. Notable times are included, such as the 70 day shutdown in 1989 (beginning on $t = 1156$ d), the first IAEA inspection in 1992 ($t = 2337$ d), and the shutdown on April 1, 1994 ($t = 3012$ d). In the leftmost panel of figure 11 we have plotted the results for case I and case II, as well as the data points found in table VIII.5 in *Nuclear Puzzle*, normalized to a 50 MTU core and we find excellent agreement. We note that immediately following the 70 day shutdown in 1989, the fissile abundances vary greatly between cases. The difference quickly disappears as the fresh fuel load is burned at a higher power so that by the first IAEA inspection in 1992 the fissile abundance differences have vanished. The results in terms of mass inventory and fission rates are shown in figure 11.

B CANDU and LEU reactors

The “H₂O, LEU” reactor and the “D₂O, NU” CANDU reactor are both calculated in the same fashion as the 5 MW_e reactor. The LEU reactor calculation is done for a typical pressurized light water reactor. Specifically, we have taken a power history from one such reactor, namely Ling Ao I, located in the Daya Bay complex in China. Ling Ao I is a Framatome M310 reactor, which uses a 17x17 AFA 3G fuel assembly. SCALE does not have this specific library, but does contain the very similar Westinghouse 17x17 array, which we have used. Details of the Ling Ao I reactor history and fuel composition are taken from the yearly power histories published via IAEA Operation Experience in Member States

documents.¹¹⁶ To summarize, Ling Ao I has a total fuel load of 72.4 MTU enriched to 3.7%. The yearly power histories are converted into OrigenArp input files. The Ling Ao I reactor runs on a 12 month refueling cycle, meaning that it must shut down about every 12 months to refuel. Typically, one third of the fuel is replaced with a fresh third, and the fuel rods are shuffled within the core to reach a flatter burn-up distribution. To simulate this, we produce three SCALE computations: one third of a core that has been irradiated once, another third that has been irradiated twice, and the last third that has been irradiated three times. These three output files are then summed resulting in the final full core. Each third has been irradiated for approximately 335 days per cycle at an average power of about 965 MW_{th}, resulting in a total power of 2.9 GW_{th}. We acquire the fission rates and the fissile abundances for the four main fissiles from this final full core sum. The “D₂O, NU” is also calculated via SCALE. We use the CANDU 37-element cross section library in SCALE. The 37-element, as opposed to the 28-element, design was chosen as it is a more common design for newer CANDU reactors. This simulation was performed with a three year irradiation time at an average power of 40 MW_{th} with a 8.6 MTU natural uranium fuel load. The CANDU reactor is run continuously with no refueling periods. From the SCALE output we obtain the fission rates and the fissile abundances for the four main fissiles. The specifications for this calculation are intended to mirror the specifications of the Arak reactor in Iran.¹¹⁷

C The IRT reactor

The IRT is a light-water pool-style research reactor and was supplied to the DPRK by the Soviet Union in the 1960s. First criticality occurred in the IRT reactor on August 15, 1965. The IRT contains 56 core grid compartments during the time of interest here, i.e. after 1986.¹¹⁸ The exact configuration of the IRT is unknown, but we can base possible

116. Mandula Jiri, “Operating Experience with Nuclear Power Stations in Member States 2005-2011,” <http://www.iaea.org/NuclearPower/Engineering/Publications/2012.html>.

117. Albright and Walrond, *Update on the Arak Reactor*.

118. Albright and O’Neill, *Nuclear Puzzle*.

configurations on similar IRT reactors such as the IRT-Sofia¹¹⁹ located in Bulgaria. These compartments can contain a driver or target element. Drivers are the primary fission source in this research reactor and are made of highly enriched uranium. The targets, which are primarily composed of fertile isotopes, such as natural uranium, will experience a small number of fissions. In 1974, the IRT was upgraded in power from 2 MW_{th} to 4 MW_{th} and later in 1986 it was upgraded from 4 MW_{th} to 8 MW_{th}. The driver element enrichment also increased during this time from 10% in 1967 to 80% by 1986.¹²⁰ Exact inventories are unavailable, but estimates indicate the DPRK may have had access to at least 92 of these 80% enriched driver elements.¹²¹ From 1986 on-wards, 30 driver elements were typically loaded and the IRT could run for about 250 days out of the year.

SCALE computations for the IRT are more difficult as there is no available cross section library provided with SCALE. Therefore, we use the Triton and NEWT modules to produce custom cross section libraries for the IRT calculations. NEWT generates the neutron transport calculation for a user-defined core configuration, which can then be used by Triton over a sample burn-up history to produce decay and cross section libraries. The input information we provide consists of detailed isotopic compositions of the driver and target elements as well as physical parameters of these elements and a core configuration. Information concerning the driver and target elements is taken from table VIII.6 in *Nuclear Puzzle*. To summarize, we are using 80% enriched U-Al alloy drivers with an aluminum cladding in a light-water moderator surrounded by a reflector. The target elements are natural uranium metal in an aluminum cladding. We utilize SCALE and the IRT power history provided in table VIII.7 in *Nuclear Puzzle* along with the initial loading of 6 kg for the drivers and 633 kg for the targets.

The actual core configuration is not known and detailed designs are unavailable so we will first determine the impact of the unknown core configuration on the fission rates, as

119. IAEA, *Directory of Nuclear Reactors*, vol. V - Research, Test and Experimental Reactors (Vienna, Austria: International Atomic Energy Agency, 1964).

120. Albright and O'Neill, *Nuclear Puzzle*.

121. Ibid.

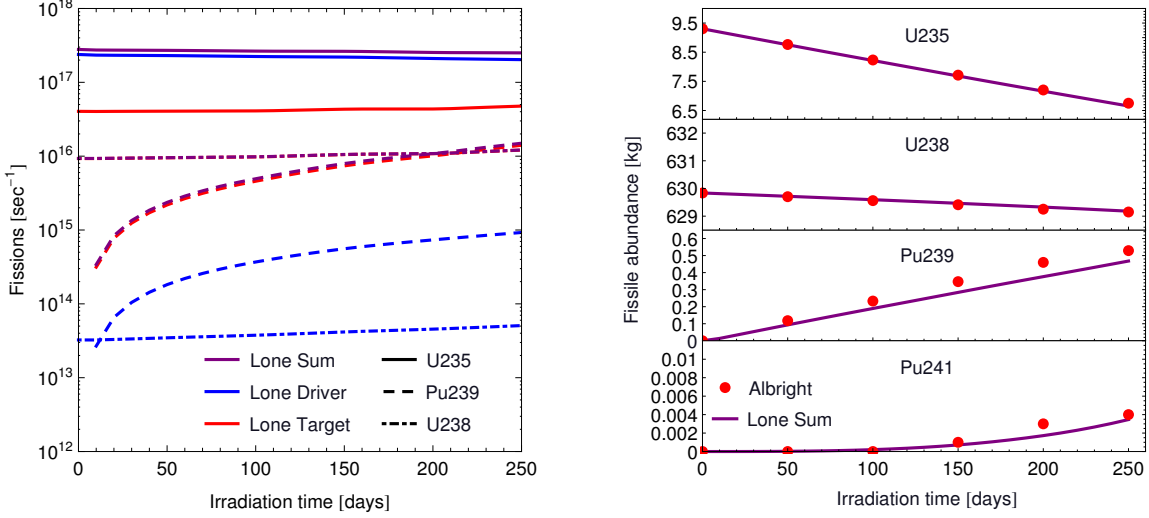


Figure 12: IRT fission rates of a lone driver and target element separately and their sum (left panel). The abundances of fissile isotopes in the IRT as calculated by the lone sum method (right hand panel).

these rates determine the neutrino spectrum. We tested several methods of computing the fission rates of the IRT research reactor. The first group of methods considered a calculation of a full IRT core with both drivers and targets present. Two core configurations were tested and are illustrated in figure 14.

The second group of methods consisted of calculating the drivers and targets separately and then summing the fission rates and fission yields for a full core. For this group we considered three sub-cases. We calculated one lone driver and one lone target separately, multiple drivers and multiple targets separately in a first core configuration and multiple drivers and multiple targets separately in a second, different, core configuration. The specific dimensions of each element and the two different core configurations can be found in figure 13 and figure 14. For the multiple drivers and targets separately we simply removed either the target or driver elements in figure 14.

The fission rates across these several methods were found to be nearly identical. The full core of both targets and drivers produced slightly higher plutonium-239 and uranium-238

fission rates. This is a result of the additional fission neutrons produced from the interplay between drivers and targets, which combines with the total neutron flux. This increase is a very small effect, especially when compared to the uranium-235 fission rate, which dominates the IRT. From this, we conclude that a specific core configuration has only a minor impact on the fission rates and we use the lone element and lone driver calculations. The primary reasoning behind this is to avoid any unverifiable core configuration bias. The fission rates for the lone element method are given in figure 12. Blue curves indicate fission rates for the driver, red curves indicate fission rates for the targets and purple curves are the sum of these. We have only illustrated the three main fissiles that contribute to the overall fission rates. The drivers comprise the majority of uranium-235 fissions and, thus, the majority of fissions over all fissiles. The addition of targets increases the plutonium-239 and uranium-238 fission rates, but these are still an order of magnitude lower than the uranium-235 fission rates. Again, we see the burn-up effect by the decreasing fission rate of uranium-235 along with an increase in the plutonium-239 fission rate.

We also wish to track the abundances of the four main fissile isotopes as a function of time over the given 250 day irradiation cycle of the IRT. The abundances have been calculated using SCALE in the same fashion as described before. We attempt three different methods, a lone driver and lone target core individually calculated and then summed, a full core with drivers and a full core with targets individually calculated and then summed, and a full core containing both drivers and targets. Again, the differences in these three methods were extremely minor resulting in the similar conclusion that the core configuration is negligible when considering the fissile abundances for the IRT. In the right panel of figure 12 we compare the fissile abundances as produced via the lone target and element separately calculated and then summed to a full core with table VIII.7 in *Nuclear Puzzle*. We find that there is an excellent match between the two results. The largest deviation occurs in plutonium-241 as there is little of this isotope being produced.

To summarize, we conclude that all methods we tested for computing the fission rates,

isotopic abundances, and neutrino fluxes for the IRT yield very similar results. The main effect in the IRT is the addition of breeding targets and we reproduce previous results in the literature.

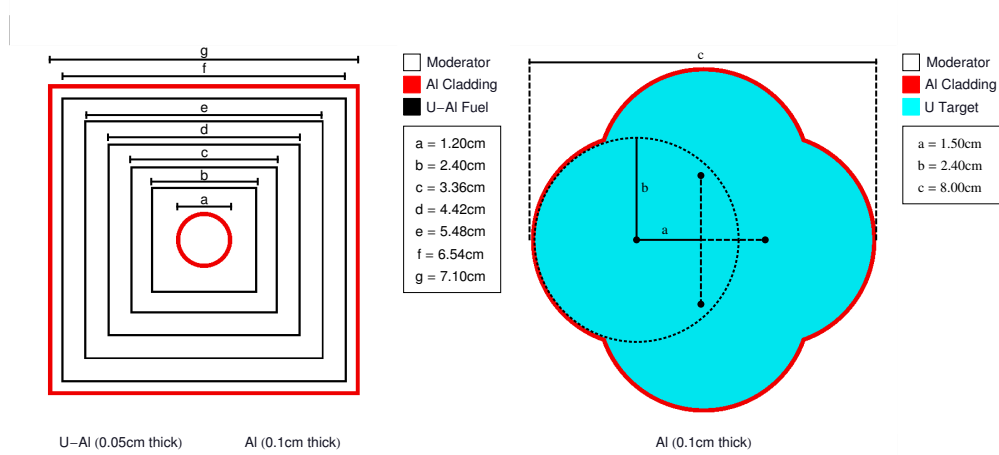


Figure 13: The left hand panel shows the IRT driver element material diagram, whereas the right hand panel shows IRT target element material diagram.

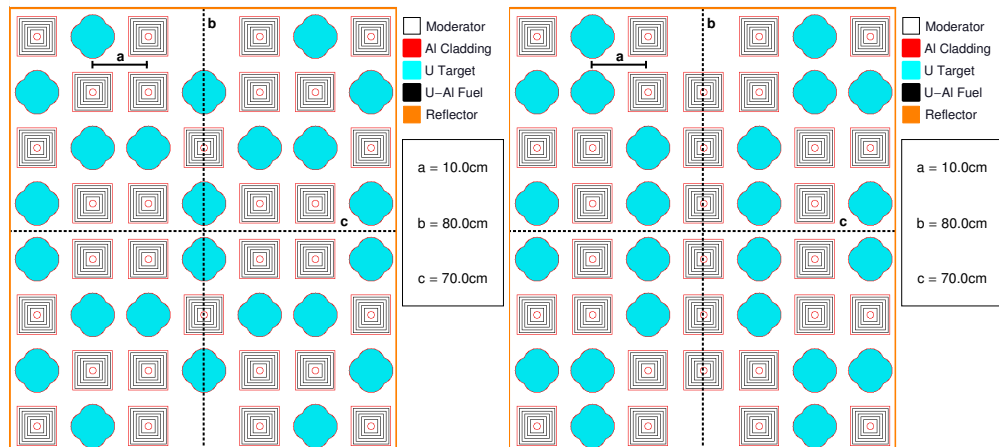


Figure 14: The left hand panel shows the IRT full core v1 material diagram, whereas the right hand panel shows the IRT full core v2 material diagram.